

1 **Modeling Seasonal Effects of River Flow on Water Temperatures in an Agriculturally**  
2 **Dominated California River**

3  
4  
5 **J. Eli Asarian<sup>1</sup>, Crystal Robinson<sup>2†</sup>, Laurel Genzoli<sup>3</sup>**

6 <sup>1</sup>Riverbend Sciences, Eureka, CA, USA, <sup>2</sup>Quartz Valley Indian Reservation, Fort Jones, CA,  
7 USA, <sup>3</sup>Flathead Lake Biological Station and the University of Montana, Missoula, MT, USA,  
8 <sup>†</sup>current affiliation: California Department of Fish and Wildlife, Yreka, CA, USA

9 Corresponding author: J. Eli Asarian (eli@riverbendsci.com)

10  
11 **Key Points:**

- 12 • In this snowmelt and groundwater-influenced river, water temperatures stayed cool later  
13 into summer in high-flow years than low-flow years
- 14 • Statistical water temperature model predictions became more accurate when the influence  
15 of river flow was allowed to vary seasonally
- 16 • These accessible models can be applied to other rivers or streams with daily, long-term  
17 flow and water temperature records
- 18  
19  
20

## 21 **Abstract**

22 Low streamflows can increase vulnerability to warming, impacting coldwater fish. Water  
23 managers need tools to quantify these impacts and predict future water temperatures. Contrary to  
24 most statistical models' assumptions, many seasonally changing factors (e.g., water sources and  
25 solar radiation) cause relationships between flow and water temperature to vary throughout the  
26 year. Using 21 years of air temperature and flow data, we modeled daily water temperatures in  
27 California's snowmelt-driven Scott River where agricultural diversions consume most summer  
28 surface flows. We used generalized additive models to test time-varying and nonlinear effects of  
29 flow on water temperatures. Models that represented seasonally varying flow effects with  
30 intermediate complexity outperformed simpler models assuming constant relationships between  
31 water temperature and flow. Cross-validation error of the selected model was  $\leq 1.2$  °C. Flow  
32 variation had stronger effects on water temperatures in April–July than in other months. We  
33 applied the model to predict effects of instream flow scenarios proposed by regulatory agencies.  
34 Relative to historic conditions, the higher instream flow scenario would reduce annual maximum  
35 temperature from 25.2 °C to 24.1 °C, reduce annual exceedances of 22 °C (a cumulative thermal  
36 stress metric) from 106 to 51 degree-days, and delay onset of water temperatures >22 °C during  
37 some drought years. Testing the same modeling approach at nine additional sites showed similar  
38 accuracy and flow effects. These methods can be applied to streams with long-term flow and  
39 water temperature records to fill data gaps, identify periods of flow influence, and predict  
40 temperatures under flow management scenarios.

41

## 42 **Plain Language Summary**

43 Warm water temperatures threaten culturally and economically important salmon in Pacific  
44 Northwest rivers, causing chronic stress and direct mortality. Climate change and agricultural  
45 water use have reduced summer river flows in recent decades, intensifying water scarcity. Years  
46 with deep mountain snowpack and resulting high groundwater levels extend the high flow season  
47 and keep water temperatures cool through the end of July, whereas in drought years the river  
48 warms sooner. We used 21 years of river flow and air temperature data from the Scott River,  
49 California, to create computer models that simulate water temperatures. Our models allow the  
50 effect of flow on water temperatures to vary by season (i.e., stronger cooling effects in spring  
51 and summer), improving accuracy of the simulated temperatures. We used the Scott River model  
52 to simulate water temperatures under two alternative flow scenarios considered in local water  
53 management plans. Our simulations indicate that relative to current conditions, the higher flow  
54 scenario would lower the summers' highest temperatures and decrease the number of days that  
55 river temperatures exceed a biological threshold. Testing the same modeling approach at nine  
56 additional Klamath Basin sites showed similar accuracy and flow effects. Our model is freely  
57 available for public use.

58

## 59 **1 Introduction**

60 Water temperature in rivers and streams drive physical, chemical, and biological processes  
61 (Ouellet et al., 2020). Stream temperatures determine species ranges, with alterations to natural  
62 temperature regimes causing deleterious effects to native species (Wenger et al., 2011). Stream  
63 temperatures are widely altered by human activities (Webb et al., 2008). Maintaining ecological

64 integrity is a major stream temperature management goal, yet models used to predict stream  
65 temperature response to management interventions either lack predictive power or are time-  
66 consuming to develop.

67 River flow rates (i.e., discharge) are a key driver of stream temperatures through multiple  
68 mechanisms. While stream temperatures are determined by surface and streambed energy fluxes  
69 and advected heat (Caissie, 2006; Moore et al., 2005), flows influence these factors and their  
70 effect on temperature. Higher flows generally increase water volume and thus a stream's  
71 capacity to store heat, reducing daily temperature fluctuations (Brown, 1969; Folegot et al.,  
72 2018; Meier et al., 2003; Sinokrot & Gulliver, 2000). Higher flows speed downstream transit of  
73 water, reducing the time that a parcel of water is exposed to ambient heating (or cooling) at a  
74 given location and increasing the influence of upstream conditions (Bartholow, 1991; Dymond  
75 J., 1984; Folegot et al., 2018). Channel geometry, including width/depth ratio, influences these  
76 effects (Dugdale et al., 2017).

77 The relationship between water temperature and flow varies through time. Seasonal changes in  
78 precipitation phase (i.e., snow and rain) affect water temperatures (Yan et al., 2021). The  
79 geographical source of water can shift seasonally, and can include tributaries, point sources,  
80 hillslopes, and alluvial aquifers, with each source having different temperatures and heating or  
81 cooling trajectories while en route to stream channels (Dugdale et al., 2017; Steel et al., 2017).  
82 Groundwater-surface water interactions and hyporheic exchange also affect temperatures  
83 (Hannah et al., 2009; Kurylyk et al., 2015). Water management, including reservoir releases,  
84 water withdrawals, and irrigation runoff can further alter temperature dynamics (Alger et al.,  
85 2021; Chandesris et al., 2019). Flow effects on water temperature are further mediated by  
86 seasonal changes to solar radiation received by the stream. Day length and solar angle, which  
87 affect topographic and riparian shading, remain consistent among years (Piotrowski &  
88 Napiorkowski, 2019; Yard et al., 2005). Other mediators of solar radiation including leaf out and  
89 leaf fall of deciduous riparian vegetation, cloud cover (Dugdale et al., 2017), water vapor, dust  
90 (Theurer et al., 1984), wildfire smoke (Asarian et al., 2020; David et al., 2018) and other aerosols  
91 follow seasonal trajectories that vary among years. Despite time-varying changes in how flow  
92 dynamics influence stream temperature, many stream temperature models do not account for  
93 these seasonal variations in the relationship between flow and stream temperatures.

94 Given stream temperature's importance and vulnerability to human alterations, water managers  
95 need tools to predict stream temperature changes associated with climate change and flow  
96 management (Gibeau & Palen, 2020; Null et al., 2017). While process-based (i.e., deterministic)  
97 models simulating stream energy budgets can have high predictive accuracy, their use is limited  
98 by extensive data input requirements (Brown, 1969; Caissie, 2006; Dugdale et al., 2017).  
99 Statistical models that use empirical relationships between stream temperature and  
100 environmental drivers require fewer input variables so are easier to implement, but for scenario  
101 prediction they are generally not considered as reliable as process-based models (Arismendi et  
102 al., 2014; Benyahya et al., 2007a; Caissie, 2006). However, statistical modeling methods have  
103 evolved, improving prediction accuracy and temporal resolution (i.e., daily) (Ouellet et al., 2020;  
104 Piotrowski & Napiorkowski, 2019). Year-round daily temperature models are especially valuable  
105 because they match the time scales used in detailed biological studies and water quality  
106 regulations (Imholt et al., 2010; Railsback et al., 2015; USEPA, 2003).

107 Statistical stream temperature models have long relied on air temperature as the primary  
108 predictor (Mohseni et al., 1998), but year-round daily models should incorporate additional

109 mechanisms to improve accuracy and reflect physical processes (Letcher et al., 2016). Statistical  
110 stream temperature models use air temperature to represent net radiative flux (Caissie 2006).  
111 Time lags between air temperatures and water temperature reflect heat exchange processes  
112 (Koch & Grünwald, 2010; Soto, 2016; Webb et al., 2003), while temporal autocorrelation  
113 acknowledges that stream temperature on a given day is in part a result of stream temperature the  
114 previous day (Benyahya et al., 2007a, 2007b, 2008; Yang & Moyer, 2020). Inclusion of flow can  
115 improve model accuracy (Santiago et al., 2017; Sohrabi et al., 2017; van Vliet et al., 2011; Webb  
116 et al., 2003). The relationship between air and stream temperatures is nonlinear and differs  
117 among seasons (Arismendi et al., 2014, Caissie et al., 2001; Mohseni et al., 1998). Including  
118 time-varying effects could improve the predictive accuracy of stream temperature models across  
119 variable conditions.

120 Several methods allow seasonal variation in the relationship between environmental covariates  
121 and stream temperatures. These methods not only improve model accuracy but also identify the  
122 times when effects are strongest. While time-varying covariate effects can be represented using  
123 separate models for each season (Mohseni et al., 1998; Sohrabi et al., 2017), this may cause  
124 unnatural, abrupt changes at seasonal transitions. Time-varying coefficients, including those used  
125 in generalized additive models (GAMs) (Pedersen et al., 2019; Wood, 2017) use continuous  
126 functions that avoid these abrupt changes (Li et al., 2014; Jackson et al., 2018; Siegel & Volk,  
127 2019). While GAMs have been used in daily stream temperature modeling for single-site  
128 prediction (Boudreault et al., 2019; Coleman et al., 2021; Glover et al., 2020; Laanaya et al.,  
129 2017; Siegel et al., 2022), spatiotemporal prediction (Jackson et al., 2018; Siegel & Volk, 2019),  
130 identifying extreme events (Georges et al., 2021), and trend assessment (Yang & Moyer, 2020),  
131 few studies have used GAMs to model seasonally varying flow effects or identify when stream  
132 temperatures are most affected by flow variation (Glover et al., 2020; Yang & Moyer, 2020).  
133 With flexible model structures and easy implementation, GAMs could be a powerful tool for  
134 predicting stream temperatures under flow management scenarios, but to our knowledge these  
135 models have not been previously used for this purpose.

136 Our objectives were to predict mean and maximum daily stream temperatures under management  
137 flow scenarios and new environmental conditions, and to identify periods when flow has the  
138 strongest influence on stream temperatures. We compared 11 GAM structures using flow, air  
139 temperature, and day of year as covariates that incorporated combinations of linear, nonlinear,  
140 and seasonally-varying effects. Our model selection and validation procedures included  
141 extrapolation tests evaluating predicted stream temperatures with flows and air temperatures  
142 outside the calibration range, designed to favor models that had enough complexity to represent  
143 the key patterns in the data, but not so complex that they overfit the data. We applied the top  
144 model to proposed management flow scenarios and extreme flow and air temperature conditions.  
145 The models are intended to be used as a tool to inform water management, making the relatively  
146 simple model structure and coding of GAMs our choice of modeling technique. We focused our  
147 analyses on the Scott River of Northern California, where low flows and high temperatures are  
148 limiting factors for coldwater fish and water managers are considering implementing regulations  
149 to protect instream flows. To demonstrate wider applicability, we evaluated similar models in  
150 nine additional sites in the Klamath River Basin.

## 152 2 Study Area

153 Our study area is the lower Klamath River Basin, California, USA, focusing on one large  
154 tributary—the Scott River (Figure 1). The Scott River study site is located at the outlet of Scott  
155 Valley, with a drainage area of 1,714 km<sup>2</sup>. The other nine sites are near USGS gaging stations  
156 with drainage areas ranging from 58 km<sup>2</sup> to 31,300 km<sup>2</sup> (Figure 1, Table S1). The climate is  
157 Mediterranean with precipitation occurring primarily in winter and spring as rain at low  
158 elevations and snow at higher elevations (VanderKooi et al., 2011). The human population lives  
159 primarily on private land along watercourses including Scott Valley, where irrigated agriculture  
160 dominates land use, utilizing groundwater and surface water (Foglia et al., 2018). The Scott  
161 River has no major dams or reservoirs, but there are large dams on the Klamath River and two  
162 tributaries (Shasta and Trinity rivers), influencing some study sites.

163 The Scott Valley aquifer fills during the high flows of winter rainstorms and spring snowmelt-  
164 driven runoff. As runoff recedes through summer, most surface water is diverted for irrigation  
165 and river water at the Scott Valley outlet becomes increasingly composed of groundwater from  
166 valley alluvium. Minimum flows occur in early September before rising due to fall rains (Figure  
167 2b). In late summer of drought years, portions of the Scott River have no surface flow (Tolley et  
168 al., 2019). Summer and fall river flows have declined in recent decades (Kim and Jain, 2010;  
169 Asarian and Walker, 2016) due to a combination of climate change (Drake et al., 2000) and  
170 increased groundwater withdrawals, especially since 1977 (Van Kirk and Naman, 2008). Climate  
171 change is expected to further reduce flows by decreasing snowpack and increasing irrigation  
172 demand (Persad et al., 2020).

173 Management flows have been proposed for the Scott River to protect Endangered Species Act-  
174 listed coho salmon (*Oncorhynchus kisutch*) and other coldwater salmonid fishes. These fishes'  
175 importance to local Native American tribes has led to contention over water management. River  
176 water temperatures in May–July are much cooler in high-flow years than low-flow years (Figure  
177 2), and water extraction has contributed to the Scott River being listed as impaired for water  
178 temperature under the Clean Water Act (NCRWQCB, 2005). The U.S. Forest Service has a first-  
179 priority Schedule D water right for Scott River instream flow that varies by month and day from  
180 30–200 ft<sup>3</sup>/s (0.85–5.67 m<sup>3</sup>/s) (Superior Court of Siskiyou County, 1980) (Figure 3b), but does  
181 not exercise its legal authority to curtail lower-priority water uses when flows drop below these  
182 levels. The California Department of Fish and Wildlife (CDFW) proposed interim Scott River  
183 instream flow targets that vary by month and day from 62–362 ft<sup>3</sup>/s (10.3–1.75 m<sup>3</sup>/s) (CDFW,  
184 2017) (Figure 3b), but these have no legal force.

185

## 186 3 Methods

187 At each of the 10 sites, we developed GAMs to predict daily mean stream temperature ( $T_{\text{mean}}$ )  
188 and daily maximum stream temperature ( $T_{\text{max}}$ ) using flow, air temperature, and day of year as  
189 covariates. We compared models across a range of complexity, including those with seasonally  
190 varying flow effects, to models with a constant relationship between stream temperature and  
191 flow. We selected a final model based on the best overall performance averaged across the 10  
192 sites. We then applied that model to flow management scenarios at one site—the Scott River.

### 193 3.1 Data sources and preparation

#### 194 3.1.1 Water temperature and river flow

195 We obtained water temperature data from six sources (Table S1). For the Scott River site, we  
 196 used Quartz Valley Indian Reservation (QVIR) (QVIR, 2016; Asarian et al., 2020) data,  
 197 supplemented by U.S. Forest Service (USFS) (KNF, 2010, 2011) and U.S. Bureau of  
 198 Reclamation (USBR) (Smith et al., 2018) data. For the nine other sites, we used data from the  
 199 U.S. Fish and Wildlife Service (USFWS) (Manhard et al., 2018; Romberger & Gwozdz, 2018),  
 200 USFS (KNF, 2010, 2011), USBR, U.S. Geological Survey (USGS), and California Department  
 201 of Water Resources (CDWR). Equipment calibration information is provided in Text S1.  
 202 Following compilation, we reviewed the data and removed any suspicious values (e.g., when  
 203 there were calibration issues or probes appear to have been exposed to air). We then calculated  
 204  $T_{\text{mean}}$  and  $T_{\text{max}}$ . For days when data were available from multiple entities, we averaged values  
 205 (Text S1). Data availability at each site ranged from 3,540–5,684 days and 16–21 years (1998–  
 206 2020), with at least five days of data for every julian day. We paired daily temperatures at each  
 207 site with daily average streamflow data from nearby USGS gages (Figure 1, Table S1).

#### 208 3.1.2 Air temperature

209 We retrieved daily mean air temperatures for each site from the 4-km resolution gridded PRISM  
 210 dataset (Daly et al., 2008). Because stream temperatures are correlated with air temperature at  
 211 multiple time scales, we initially explored many metrics (Piotrowski & Napiorkowski, 2019). In  
 212 these initial explorations at Scott River, we found that two-day weighted air temperature ( $A_{2w}$ )  
 213 resulted in good model fits (Text S2), so we used  $A_{2w}$  for all models except one that used a  
 214 seven-day average ( $A_7$ ) to mimic Mohseni et al.’s (1998) widely-implemented model.  $A_{2w}$  is  
 215 calculated as follows, where  $A$  is mean air temperature on day  $i$ :

$$216 \quad A_{2w} = \frac{A_i + (0.5 \times A_{i-1})}{1.5} \quad (1)$$

217  
 218 To improve numerical stability, we standardized air temperature ( $^{\circ}\text{C}$ ) and flow ( $\log_{10} \text{ m}^3/\text{s}$ ) by  
 219 centering and scaling (i.e., subtracting the mean, then dividing by the standard deviation).

220

#### 221 3.1.3 Flow and air temperature quantiles

222 At each site, we used smooth additive quantile regression models (Cade and Noon, 2003; Fasiolo  
 223 et al., 2020) to calculate the air temperature associated with three quantiles (0.1, 0.5, and 0.9,  
 224 equivalent to 90%, 50%, 10% exceedance probabilities) for each day of the year (Figure 3a),  
 225 using the qgam R package (Fasiolo et al., 2020) with a 12-knot cyclic cubic regression spline  
 226 (“cc”). We refer to the 0.1, 0.5, and 0.9 air temperature quantiles as Coolest, Typical, and  
 227 Hottest, respectively. We also derived three flow quantiles, with the 0.1 quantile representing  
 228 Lowest flows, 0.5 quantile representing Typical flows, and the 0.9 quantile representing Highest  
 229 flows (Figure 3b). These quantiles were used to generate model scenarios (Section 3.4).

230 We used similar quantile regression models at each site to categorize each date into one of nine  
 231 categories based on combinations of flow quantiles (High is  $>0.67$  quantile, Moderate is  $0.33$ –  
 232  $0.67$  quantile, Low is  $<0.33$  quantile) and air temperature quantiles (Cool is  $<0.33$  quantile,

233 Moderate is 0.33–0.67 quantile, Warm is > 0.67 quantile). These categories were used to define  
234 cross-validation blocks (Section 3.3).

235

### 236 3.2 Model development and calibration

237 At each of the 10 sites, we developed 11 models of  $T_{\max}$  and  $T_{\text{mean}}$  using combinations of river  
238 flow, air temperature, and day of year (D) as covariates, including interactions (Figure 4).  
239 Models are numbered according to effective degrees of freedom for fixed effects, from most  
240 complex (GAM1) to least complex (GAM11). GAMs were developed in the *mgcv* R package  
241 version 1.8-41 using the *bam* function (Wood, 2017), fit using fast restricted maximum  
242 likelihood (fREML). Model terms were either linear coefficients or smooth non-linear functions  
243 with wiggleness determined by a smoothing penalty (Pedersen et al., 2019; Wood, 2017). We  
244 used cyclic cubic regression splines (“cc”) as the smoother for D and thin plate regression splines  
245 (“tp”) as smoothers for other covariates. To improve prediction under new conditions and avoid  
246 overfitting (Jackson et al., 2018; Siegel & Volk, 2019), we limited smoothers for air temperature  
247 and flow to a maximum of three knots, except in the one-covariate model “GAM11” where air  
248 temperature was allowed six knots. D was allowed up to six knots, except in three-dimensional  
249 tensors where it was restricted to five knots.

250 Some models included interactions between D and other covariates (i.e., flow or air temperature)  
251 to allow that covariate’s effect to vary seasonally. These interactions were either partially  
252 nonlinear or fully nonlinear. For partially nonlinear interactions, the linear slope of one variable  
253 (e.g., flow) varied as a smooth nonlinear function of D (Jackson et al., 2018, Siegel & Volk,  
254 2019). Fully nonlinear relationships between two or more variables were specified as tensor  
255 product smooths or tensor product interactions (Wood, 2017).

256 All models except “GAM11”, the simplest model structure tested, included an AR-1  
257 autocorrelation error structure and a random effect for year. We initially fit each model without  
258 an autocorrelation term, then re-fit with an autocorrelation term, assigning a rho value based on  
259 the initial model’s lag-1 autocorrelation (Baayen et al., 2018; van Rij et al., 2019, 2020) (Text  
260 S3).

261 Since Mohseni et al.’s (1998) nonlinear logistic regression of weekly air temperature and stream  
262 temperature has been widely applied and adapted (Piotrowski & Napiorkowski, 2019), we  
263 included a GAM equivalent of it as a benchmark for comparison.  $A_7$  is the only predictor in this  
264 “GAM11” model (i.e., no flow, autocorrelation, or random effects).

265 We reviewed residual plots and autocorrelation function plots to verify assumptions. We  
266 evaluated each model’s concurvity using *mgcv*’s concurvity function.

267

### 268 3.3 Model selection and validation

269 We used cross-validation (CV) for model selection and validation because it is preferred over  
270 information theoretic approaches when prediction is paramount (Pedersen et al., 2019). We  
271 designed extrapolation CV tests to select models that performed well when applied to  
272 environmental conditions (i.e., flow and air temperature) outside the calibration range (Lute &  
273 Luce, 2017; Roberts et al., 2017). We split data into blocks based on quantiles of flow and air

274 temperature (Section 3.1.3), withheld one block, and fit the model using the remaining block  
275 (Figure 5). We compared predictions for the withheld blocks against the measured data using  
276 root mean squared error (RMSE). These dual-variable differential split-sample tests (Klemeš,  
277 1986) extrapolate not only into new combinations of flow and air temperature but also into new  
278 ranges of both individual variables.

279 We selected the best model by ranking the 11 candidate models (GAM1–GAM11) based on their  
280 extrapolation test RMSE values for each site and each temperature response variable (10 sites, 2  
281 variables). We then calculated the mean of the 20 ranks for each candidate model, selecting the  
282 model with the lowest mean rank. We selected the same model structure for  $T_{\max}$  and  $T_{\text{mean}}$   
283 (rather than optimizing separately) so predictions for both metrics could be used together. We  
284 present Bayesian information criterion (BIC) scores from models fit using maximum likelihood,  
285 to compare our extrapolation-based model selection to more commonly applied—and easier to  
286 implement—model selection methods. To facilitate comparisons to previous studies, we also use  
287 leave-one-year-out (LOYO) CV where data were split into annual blocks and then treated  
288 similarly to the extrapolation tests (i.e., steps repeated for each year: year withheld, model refit  
289 using remaining data, and predictions compared to withheld data). We assessed the relative  
290 importance of individual model terms by comparing performance among models with and  
291 without individual predictors and/or interactions.

292

### 293 3.4 Model scenarios assessing management effects and timing of flow importance

#### 294 3.4.1 All sites

295 To assess the seasonal response of stream temperatures to variation in flow and air temperatures,  
296 we applied our selected model to scenarios representing differing air temperatures and flows  
297 (Table 1, Figure 3). We ran nine “quantile air temperature” scenarios representing combinations  
298 of three air temperature inputs (0.1, 0.5, and 0.9 quantiles) and three flow inputs (0.1, 0.5, and  
299 0.9 quantiles) (Section 3.1.3) for each site. Replication is sparse for the co-occurrence of extreme  
300 quantiles of both air temperature and flow (e.g., mean 4.9 days of record per month and site with  
301 flow  $\leq 0.1$  quantile and air temperature  $\geq 0.9$  quantile); however, ample data are available in  
302 nearby quantiles (e.g., mean 19.1 days per month and site with flow  $\leq 0.2$  quantile and air  
303 temperature  $\geq 0.8$  quantile) (Figure S1).

304

#### 305 3.4.2 Scott River

306 At Scott River only, six additional scenarios were run that paired the three quantile air  
307 temperatures with the USFS water right and CDFW flow criteria (Section 2) as flow inputs  
308 (Table 1, Figure 3). The CDFW and USFS flows are aligned with extreme drought conditions in  
309 April and May (0.1 quantile) and high flows in August and September (0.5 to 0.9 quantile).

310 We also applied our selected model to “observed air temperature” scenarios that pair observed  
311 air temperatures for dates 1998–2020 with eight flow conditions for the Scott River: observed  
312 USGS flows, the five flows from the “quantile air temperature” scenarios (Lowest, Typical,  
313 Highest, USFS, and CDFW), and two additional scenarios in which the CDFW and USFS flows  
314 were replaced by observed USGS flows on dates when the observed flows were higher than the

315 management flows (Table 1). Using observed air temperatures instead of quantile air  
316 temperatures provides more realistic predictions because air temperatures fluctuate from day to  
317 day (Figure 2a), instead of remaining near the same quantile like flow does during May–  
318 September recession. We summarized the results of each “observed air temperature” scenario by  
319 calculating: 1) annual maximum temperature, 2) first and last day each year in which water  
320 temperatures exceed 22 °C, and 3) the annual degree days exceedance of 22 °C, calculated by  
321 subtracting 22 from all  $T_{\max}$  and summing all positive values. We chose 22 °C as an indicator of  
322 biological effects on juvenile salmonids, based on geographically proximal studies (Brewitt and  
323 Danner, 2014; Sutton et al., 2007; Sutton & Soto, 2012) (Text S4).

324  
325

## 326 **4 Results**

### 327 4.1 Model selection and validation

328 GAM7 had the lowest mean rank RMSE in extrapolation CV (Table S2), so was selected as our  
329 final model. GAM7 had an all-site RMSE of 1.15 °C for  $T_{\max}$  and 1.01 °C for  $T_{\text{mean}}$ , and had the  
330 lowest RMSE at Scott River ( $T_{\max}$  1.20 °C,  $T_{\text{mean}}$  1.00 °C) (Figure 4). GAM7 features nonlinear  
331 smoothers for day of year (D), two-day weighted air temperature ( $A_{2w}$ ), and flow (Q); a  
332 nonlinear smoother of D interacted with linear Q (i.e., linear slope of Q varies by D); and a  
333 nonlinear smoother of D interacted with linear  $A_{2w}$  (Figure S3, Figure 6). GAM7 had  
334 intermediate complexity, with 12.6 effective degrees of freedom for fixed effects for Scott River  
335  $T_{\max}$ , compared to 23.6 for the most complex model (GAM1), and 5.8 for the least complex  
336 model (GAM11) (Figure S4).

337 Extrapolation CV showed that at all sites, including Scott River, models with seasonally varying  
338 flow effects had much higher accuracy than models lacking that feature (Figure 4). For example,  
339 for  $T_{\max}$ , all-site RMSE was 1.15–1.19 °C for models with seasonally-varying flow effects  
340 (GAM1–GAM8) and 1.67 °C for GAM9 that lacked seasonally varying flow. Models lacking  
341 flow (i.e., containing only D or  $A_{2w}$ ) performed the worst, with all-site RMSE values of 1.74 °C  
342 and 2.25 °C for GAM10 and GAM11, respectively, for  $T_{\max}$ . GAM7’s combination of a  
343 nonlinear smoother for flow and a partially nonlinear interaction of flow and D represented flow  
344 effects well, given that the additional complexity of tensors (fully nonlinear interactions of flow  
345 and D) in GAM1–GAM5 did not substantially improve model performance at most sites. Models  
346 interacting flow and air temperature (i.e., GAM1 and GAM4) did not outperform GAM7 which  
347 lacked this interaction. BIC scores largely corroborate the extrapolation CV results identifying  
348 the importance of seasonally varying flow effects and top ranking of our extrapolation CV-  
349 selected model GAM7 (Text S5, Figure S4).

350 Scott River GAM7 LOYO CV predicted overall seasonal patterns in measured  $T_{\max}$  for dates  
351 stratified into combinations of differing quantiles of air temperatures and flows. RMSE was  
352 higher for dates with low (<0.33 quantile) flows (Figure S2c).  $T_{\max}$  Scott River GAM7  
353 extrapolation CV prediction accuracy was only slightly lower than LOYO CV prediction  
354 accuracy when averaged over the entire year (i.e., RMSE 1.20 °C vs. 1.18 °C, Figure 4), but  
355 were biased low during May and June during high (>0.67 quantile) flows, having only been  
356 calibrated with data from the low-flow and moderate-flow quantile (Figure S5). Complete time  
357 series of Scott River measured and LOYO CV  $T_{\max}$  and  $T_{\text{mean}}$  for all years are shown in Figures  
358 S6–S7.

359

## 360 4.2 Model scenarios assessing management effects and timing of flow importance

361 Water temperature predictions under quantile air temperature scenarios on the Scott River using  
362 our selected model (GAM7) showed water temperatures responded to changes in flow across all  
363 quantiles of air temperature, consistent with measured data (Figure S2). Cooling effects of flow  
364 followed a seasonal pattern, rising in March to reach maximum effect size on 15 June (7.7 °C for  
365  $T_{\max}$  and 5.5 °C for  $T_{\text{mean}}$ ), then diminishing to near zero by early September (Figure 7).

366 Consistent with measured data (Figure S2), modeled annual maximum water temperatures  
367 occurred later in the season in high-flow conditions (i.e., late July or early August) than in low-  
368 flow conditions (i.e., early/mid-July) (Figure 7).

369 Timing and magnitude of flow effects varied among the 10 Klamath Basin sites, but generally  
370 followed a similar seasonal trend of flow having the strongest cooling effects in April–July, less  
371 cooling effects in March and August, and warming effects in November through February  
372 (Figure 8). Cooling effects of flow were strongest at Scott River and weakest at Shasta River.

373 The Scott River “observed air temperature” scenarios, which paired observed air temperatures  
374 with eight flow scenarios, demonstrated how flow variation influences stream temperature timing  
375 and magnitude. The lowest flow scenario (0.1 quantile) had annual maximum temperatures 3.3  
376 °C warmer than the highest flow scenario (0.9 quantile) (Figure 9a), and first reached 22 °C 48  
377 days earlier (Figure 9c). The last day with temperatures >22 °C differed by only 2 days (Figure  
378 9d). The observed scenario had the most interannual variation in annual maximum temperature  
379 (Figure 9a) and timing of exceedances of 22 °C (Figure 9c,d), because it included very low flows  
380 and very high flows. Predicted temperature responses to the CDFW and USFS flow scenarios are  
381 complex and depend on how the flows are implemented. If implemented as bypass flows, above  
382 which all additional water is diverted, then temperatures reached 22 °C *earlier* than the observed  
383 flow scenario by 4 days for the CDFW flows and 13 days for USFS flows (Figure 9c and Figure  
384 S8) because these management flows are lower than observed flows in May and June (Figure 3).  
385 However, in the scenarios where the CDFW and USFS flows were replaced by observed USGS  
386 flows on dates when the observed flows were higher than the management flows, then predicted  
387 temperatures reached 22 °C *later* than the observed scenario by 4 days with CDFW flows and 2  
388 days with USFS flows. In addition, the number of years with exceedances of 22 °C prior to 23  
389 June were reduced from 7 to 0 (Figure 9c) because CDFW flows were higher than observed  
390 flows in drought years. Due to higher July and August flows, annual maximum water  
391 temperatures were 1.0–1.1 °C cooler in the CDFW scenarios than the observed flow scenario  
392 (Figure 9a). Differences in annual degree-days exceedance of 22 °C between scenarios (Figure  
393 9b) were similar to annual maximum temperature.

394

395 **5 Discussion**

396 At all 10 sites, models with seasonally varying flow effects substantially outperformed models  
397 with a constant relationship between stream temperature and flow, indicating that the influence  
398 of flow changes throughout the year. Models containing only air temperature performed  
399 particularly poorly because they did not include flow as a covariate, while models with a linear  
400 effect of flow had intermediate accuracy. Flow had the strongest effect on water temperatures in

401 April–July. The highest Scott River management flow evaluated would substantially decrease  
402 exceedances of 22 °C and reduce annual water temperature maximums.

### 403 5.1 Model selection and performance

404 Model accuracy of our top model and similar model structures were high for both  $T_{\max}$  and  $T_{\text{mean}}$ .  
405 For  $T_{\text{mean}}$ , our selected model's LOYO CV RMSE ranged from 0.80–1.17 °C at 10 sites (Figure  
406 4), better than the 0.75–1.75 °C RMSE in Mohseni-based models at 14 sites within our study  
407 area (Manhard et al., 2018). In addition to outperforming other models applied within our study  
408 area, our selected  $T_{\text{mean}}$  model also had better LOYO CV RMSE than most single-station year-  
409 round daily statistical models from around the world (all-site average model validation RMSE  
410 for each analysis's best performing class of models: Ahmadi-Nedushan et al. [2007] 0.51 °C,  
411 Boudreault et al. [2019] 1.45 °C, Coleman et al. [2021] 1.3 °C, Koch and Grünwald [2010] 1.25  
412 °C, Laanaya et al. [2017] 1.44 °C, Letcher et al. [2016] 1.16 °C, Siegel et al. [2022] 0.87 °C,  
413 Sohrabi et al. [2017] 1.25 °C, van Vliet et al. [2011] 1.8 °C, and Soto et al. [2016] 1.20 °C). Our  
414 high model accuracy was achieved despite using PRISM air temperatures instead of local  
415 measurements—favoring ease of replicability.

416 GAMs were a useful modeling approach because they represented the nonlinear relationships  
417 and interactions between stream temperature and covariates. Our approach used >15-year  
418 calibration datasets spanning environmental conditions (i.e., hot and cool air temperatures and  
419 high and low flows). We prevented overfitting by restricting the number of knots in GAM  
420 smoothers (Section 3.2), basing model selection on extrapolation tests that evaluate prediction  
421 under expanded ranges of covariates (Section 3.3), and confirming that covariate responses and  
422 interactions matched scientific hypotheses regarding underlying physical processes (Section 5.3).  
423 Our selected model, GAM7, represented flow with two terms—a nonlinear smoother and a  
424 partially nonlinear interaction between flow and day of year—whose combined effects (Figure 6)  
425 provided enough flexibility for accurate predictions without overfitting. This two-term structure  
426 incrementally improves upon previous methods for representing flow effects, with GAM7's all-  
427 site extrapolation CV RMSE 0.04 °C better than GAM6, the model with a simpler flow effects  
428 structure nearly identical to Glover et al. (2020). Consistent with warnings from Siegel & Volk  
429 (2019), tensors (fully nonlinear interactions) were too flexible and did not perform as well as  
430 GAM7 when applied to conditions differing from the calibration dataset (i.e., extrapolation  
431 tests), although tensor models still outperformed models without seasonally varying flow effects.

432 We used extrapolation CV for model selection, which required far more effort than BIC-based  
433 selection. Since BIC scores suggested selection of the same model, GAM7 (Text S5), from an  
434 ease-of-use perspective BIC-based model selection appears preferable for future applications.  
435 However, for applications requiring high confidence in model accuracy, the extrapolation tests  
436 effectively demonstrate the ability to predict under new conditions.

437

### 438 5.2 Magnitude and timing of flow effects on water temperature

439 Consistent with physical expectations, our results corroborate previous findings from northern  
440 temperate rivers that during seasons when air temperatures are typically high and flows are  
441 typically low (i.e., summer in our study area), lower flows are often temporally correlated with  
442 higher stream temperatures (Arora et al., 2016; Isaak et al., 2017; Luce et al., 2014; Neumann et  
443 al., 2003), and flow more strongly affects  $T_{\max}$  than  $T_{\text{mean}}$  (Asarian et al., 2020; Gu and Li, 2002;

444 Gu et al., 1998). In our study streams, high flows had a strong cooling effect on stream  
445 temperatures in April–July, but less influence during other months. Multiple linear regression  
446 (MLR) models using monthly flow and air temperature at 239 Northwestern USA sites not  
447 regulated by dams (Isaak et al., 2018) and spatial stream network models for eight regions of the  
448 Western USA (FitzGerald et al., 2021) showed monthly timing and direction of flow effects on  
449 stream temperatures (Figures S9–S10) similar to our results (Figure 8b), with the exception of  
450 similar cooling in April and August whereas our models show weaker cooling in August than in  
451 April. Monthly MLR modeling in 17 sites in Canada’s Frasier River Basin found flow-mediated  
452 cooling effects on summer water temperatures were stronger in July than August and weakest in  
453 September (Islam et al., 2019). In Poland, where inter-season flow differences are less  
454 pronounced than in our study area, high flows were correlated with cooler water temperatures in  
455 April–September, with the strongest relationships occurring in July–September at mountainous  
456 snowmelt-fed rivers (Wrzesiński and Graf, 2022). An Eastern USA river study using a daily  
457 year-round GAM found that water temperature decreased with increased flow from April  
458 through mid-October (Yang & Moyer, 2020). Previous studies evaluating year-round changes in  
459 the relationship between stream temperature and flow generally used monthly time steps. Our  
460 daily model provides a more nuanced understanding of seasonal dynamics by allowing this  
461 relationship to change smoothly at sub-monthly time scales, facilitating identification of changes  
462 within a month, as well as the rate of change.

463 Flow-induced cooling in snowmelt-dominated rivers is common. Process-based modeling of a  
464 Sierra Nevada river indicated early summer stream temperatures up to 16 °C cooler in a record  
465 wet year relative to a dry year (Null et al., 2013). In steep Alaskan streams, average summer  
466 stream temperatures were 3–5 °C cooler in high-snowpack years than low-snowpack years (Cline  
467 et al., 2021). In the conterminous USA, including flow as a covariate improved daily stream  
468 temperature predictions over air temperature only models in April–August, but only in  
469 snowmelt-dominated streams (Sohrabi et al., 2017). Stronger flow effects occurred in inland  
470 regions than coastal regions of the Western USA (Figure S10) (FitzGerald et al., 2021),  
471 consistent with a greater percent of precipitation falling as snow (Klos et al., 2014). Climate  
472 change studies have not parsed the separate influences of hydrology and air temperature on  
473 stream temperature, but in snowmelt-dominated areas of western North America, predictions for  
474 disproportionate spring and summer stream temperature warming are nearly ubiquitous and  
475 attributed to snowpack declines causing lower flows in those seasons (Caldwell et al., 2013;  
476 Crozier et al., 2020; Ficklin et al., 2014; Leach & Moore, 2019; Lee et al., 2020; Luo et al., 2013;  
477 Null et al., 2013).

478

### 479 5.3 Model correspondence to physical mechanisms

480 We used air temperature and flow as the major predictors in our model, recognizing that these  
481 predictors represent many processes that collectively determine stream temperatures. Air  
482 temperature is not the most important component of stream heat budgets (Johnson, 2004;  
483 Dugdale et al., 2017), but it has high predictive power because it is correlated with net radiative  
484 flux, a key driver of stream heat budgets (Caissie 2006). Air temperature data resulted in high  
485 model accuracy in our study, and are widely attainable unlike radiative fluxes.

486 The effects of flow on stream temperature vary throughout the year in response to the physical  
487 mechanisms affecting stream energy balances. High flows speed downstream transit of water and

488 provide increased thermal mass that resists heating (or cooling). While flow has strong effects on  
489 water temperature in April–July in our study area, its effects are substantially weaker—though  
490 still present—in August. High flow can exert a dominant influence on water temperature, but this  
491 influence wanes as flow recedes, leading to progressively greater influence of solar radiation and  
492 air temperature. The relationship between flow and water temperature in our top-performing  
493 model is nonlinear and varies with day. Marginal effects of decreasing flow diminish as flow  
494 approaches 0 m<sup>3</sup>/s (Figure 6). At Scott River, August flows were much lower than July (Figure 2,  
495 Figure 6), and by 15 August were always below 2.6 m<sup>3</sup>/s (92 ft<sup>3</sup>/s). These low August flows have  
496 shallow water depth, low thermal mass, and slow transit times resulting in residence time  
497 sufficient for water to heat up to equilibrium temperature (Bogan et al., 2003; Nichols et al.,  
498 2014; Tague et al., 2007). During hot, dry conditions such occurs in our study area during  
499 summer, evaporative cooling limits how high stream temperatures can rise even when flows are  
500 extremely low (Mohseni & Stefan, 1999; Mohseni et al., 1998; Shaw et al., 2017). Wildfire  
501 smoke could also reduce warming of August stream temperatures (David et al., 2018).  
502 Widespread fire is more likely during drought conditions (Westerling, 2016), suggesting  
503 potential for smoke to confound low flow effects on temperature by decreasing solar radiation.  
504 We did not include smoke in our models because the data are difficult to process and we wanted  
505 easily replicable methods, but smoke effects on stream temperatures peaked in August in our  
506 study area (Asarian et al., 2020). With less solar radiation and cooler air temperatures than earlier  
507 months,  $T_{\max}$  is almost always less than 22 °C at Scott River by early September regardless of  
508 flow (Figure 7). In October–November, a period of hydrologic transition when precipitation ends  
509 seasonal baseflow recession, flows had little influence over stream temperature (Figure 8), but  
510 Scott River and two other sites had weak, modal flow-temperature relationships (i.e., highest  
511 water temperatures at moderate flows) (Text S6).

512 Groundwater contributes to the relationship between flow and stream temperature at our Scott  
513 River site, as it does in many rivers (Briggs et al., 2018; Isaak et al., 2017; Kelleher et al., 2012;  
514 Mayer, 2012; Nichols et al., 2014). Thermal infrared imagery, field measurements (NCRWQCB,  
515 2005), and a groundwater model (Tolley et al., 2019) confirm that the 10 km of river directly  
516 upstream of our study site are a gaining reach where valley constriction forces substantial  
517 groundwater into the Scott River, a common phenomenon at the outlet of alluvial valleys  
518 (Stanford and Ward, 1992). Scott River flows are driven by a mix of valley groundwater  
519 dynamics and snowmelt-driven mountain runoff (Foglia et al., 2013; Van Kirk and Naman,  
520 2008). As mountain runoff recedes and tributaries are almost fully diverted for irrigation, the  
521 relative contribution of groundwater to surface flow at the valley outlet increases over the  
522 summer and becomes dominant (NCRWQCB, 2005). Sediments underlying the river and its  
523 tributaries have high hydraulic conductivity, so groundwater and surface water are strongly  
524 connected (Tolley et al., 2019). During the May–September recession period when temperatures  
525 are of greatest biological concern, flows are related to aquifer levels, and the relative proportions  
526 of valley outlet flow derived from mountain runoff and groundwater are well-predicted by flow  
527 and day of year. Thus, even though these two sources have different temperatures and our model  
528 does not explicitly differentiate them, the model performs well because the interaction of flow  
529 and day of year implicitly characterizes these dynamics adequately. Scenarios from a short-term  
530 process-based surface water model predicted doubling groundwater-derived flow would cool 30  
531 July 2003 Scott River  $T_{\max}$  by 2 °C, and a 50% reduction of groundwater-derived flow would  
532 warm temperatures by 2 °C (NCRWQCB, 2005). For comparison, applying our model to

533 scenarios doubling or halving the 3.03 m<sup>3</sup>/s (107 ft<sup>3</sup>/s) gaged flow for that same date predicts  
534  $T_{\max}$  1.0 °C cooler or 0.7 °C warmer, respectively.

535 Statistical models typically require many fewer variables as data inputs than process-based  
536 models do, so are often much simpler to develop (Caissie, 2006; Ouellet et al., 2020); however,  
537 this ease has tradeoffs. For example, our model does not differentiate between specific sources of  
538 inflows, which may have quite different temperature influences, nor how alternative  
539 management scenarios would spatially and temporally alter those inflows. If fundamental  
540 characteristics of valley hydrology (i.e., management or climate) changed dramatically, model  
541 accuracy could suffer. Similarly, applying the model to covariate combinations beyond those  
542 used in calibration will degrade predictive accuracy (Section 5.5). To avoid overly complex  
543 models that overfit calibration data, we used extrapolation tests to favor selection of simpler  
544 more generalizable models. Our model does not incorporate longer-term (e.g., annual to decadal)  
545 variation in air temperature that affects groundwater temperatures and precipitation phase (e.g.,  
546 snow or rain), so may underestimate responses relative to predictions from integrated process-  
547 based models (Leach & Moore 2019).

548

#### 549 5.4 Biological implications

550 Higher Scott River flows extend the period when cool water habitat is available (Figure 9),  
551 giving juvenile salmonids additional time to migrate downstream and reduce thermal stress for  
552 fish that rear in the Scott River through the entire summer. Climate change will likely continue to  
553 reduce snowpack and summer flows (Persad et al., 2020), increasing duration of detrimentally  
554 warm temperatures. Mean diel range in June–August exceeds 5 °C, providing hours daily with  
555 temperatures <22 °C even when  $T_{\max}$  exceeds 22 °C. Salmonids can potentially persist by using  
556 thermal refugia where cool tributaries, groundwater, or hyporheic flow enters the river during  
557 hotter hours and then forage in the mainstem when temperatures are cooler (Brewitt and Danner,  
558 2014; Sutton et al., 2007; Sutton & Soto, 2012). However, substantial portions of the Scott River  
559 and tributaries lack surface flow during summer, especially in dry years, reducing habitat  
560 connectivity.

561

#### 562 5.5 Applications and management implications

563 These models can be used not only to identify the seasonally varying influence of flow, but also  
564 to predict future stream temperatures based on managed flow recommendations and to impute  
565 missing data. Instream flow management frameworks are evolving (Mierau et al., 2017; Poff et  
566 al., 2017; Yarnell et al., 2020) and accurate stream temperature models provide a valuable tool to  
567 predict management outcomes.

568 Our modeling approach could facilitate water managers' ability to include stream temperature as  
569 a management target in areas that do not currently have operational process-based models. For  
570 example, Siskiyou County is developing a groundwater sustainability plan for the Scott Valley  
571 (Foglia et al., 2018). The current groundwater model does not simulate water temperatures  
572 (Tolley et al., 2019). Our model can be used to predict effects of flow on Scott River  
573 temperatures, including the CDFW and USFS flow thresholds under consideration, and could  
574 inform state agencies' development of new flow objectives. The CDFW and USFS flows were

575 both predicted to cool maximum annual temperatures relative to current conditions, but  
576 improvements would be greater with the higher CDFW flows (Figure 9). We caution that while  
577 the CDFW and USFS flows are higher than typical observed flows in late summer and early fall,  
578 for March to early June they represent extreme drought conditions that could cause earlier  
579 exceedances of 22 °C (Figure 2b). Surface water diversions for in lieu recharge (switching  
580 irrigation source from groundwater to surface water) or managed aquifer recharge (Dahlke et al.,  
581 2018; Foglia et al., 2013) should not use the CDFW and USFS flows to guide maximum  
582 diversion rates, but instead be tailored to reduce deleterious effects on instream habitat including  
583 temperatures, such as ceasing diversions by 1 June, the first date when measured (Figure 2) and  
584 modeled temperatures (Figure 9) reach 22 °C.

585 As with any statistical model, prediction accuracy will degrade when applied to conditions more  
586 extreme than those present in the calibration dataset. Our selected model interacts day of year  
587 with flow and air temperature, so extrapolation caution applies not just to the range of individual  
588 variables but also their combined distributions. Our calibration dataset includes a wide range of  
589 hydrologic conditions, but no years without surface water diversions or groundwater pumping  
590 because those activities occur every year. Streamflow depletion from groundwater pumping is  
591 greater in dry years than wet years (Foglia et al., 2013). Simulated total valley-wide streamflow  
592 depletion peaks around 150,000 m<sup>3</sup>d<sup>-1</sup> (60 ft<sup>3</sup>/s) in July–August (Foglia et al., 2013), exceeding  
593 streamflow in dry years. Our model should be suitable for modeling dry years for scenarios with  
594 reduced pumping and/or diversions, which would presumably have flows similar to existing wet  
595 years (and hence are within the range of calibration flows); however, in wet years such scenarios  
596 would likely exceed the range of calibration flows and therefore be subject to more uncertainty.  
597 Future application to scenarios with flows higher than observed should be interpreted with  
598 appropriate caveats.

599 Flow records are typically less available than water temperature records, so may constrain where  
600 our modeling approach can be applied. However, if site-specific flows were not available, data  
601 from a nearby site could be used if they were likely to be highly correlated (i.e., similar  
602 watershed characteristics). We did not systematically explore that issue, but the one site (South  
603 Fork Trinity River) where we used flows from an upstream station had prediction accuracy  
604 similar to the other nine sites (Figure 4). In addition, although our modeling approach should  
605 work well with records shorter than the >15-year datasets we used, we recommend further  
606 research to determine the minimum required period of record.

607 These models can also be used to fill gaps in stream temperature data records needed for other  
608 analyses (Glover et al., 2020). Their high accuracy suggests they would compare well with  
609 imputation methods used in recent daily year-round stream temperature analyses (Isaak et al.,  
610 2020; Johnson et al., 2021).

611

## 612 **6 Conclusions**

613 Long-term daily stream temperature datasets enabled development of generalized additive  
614 models (GAMs) that include nonlinear and seasonally varying effects of flow and air  
615 temperature on stream temperature. Cross-validation indicated these models had higher accuracy  
616 than models that did not account for seasonally variable effects of flow, providing evidence that  
617 flow is important in controlling stream temperatures and that the influence of flow is variable

618 through time. Results from these models indicated that high river flow had a strong cooling  
619 effect on river temperatures during April through July at 10 sites in the Klamath Basin of  
620 California, corroborating similar findings from western North America.

621 Results from extrapolation cross-validation tests show that our selected model is robust in  
622 estimating stream temperatures under environmental conditions moderately outside of the range  
623 of conditions used to train the model (although see cautions in Section 5.5). We applied the  
624 model to instream flow management scenarios proposed by regulatory agencies at our focal  
625 study site, the Scott River, finding that these scenarios would improve stream temperatures.  
626 Relative to historic conditions, the higher instream flow scenario would reduce annual maximum  
627 temperature from 25.2 °C to 24.1 °C, reduce annual exceedances of 22 °C (a cumulative thermal  
628 stress metric) from 106 to 51 degree-days, and delay onset of water temperatures >22 °C during  
629 some drought years.

630 These models contribute to an emerging body of work demonstrating the use of GAMs for  
631 predicting daily river temperatures. Our models are easy to implement and improve prediction  
632 accuracy of stream temperature responses to flow changes over models without seasonally  
633 variable effects of flow, providing tools that managers can use to select flow solutions most  
634 likely to protect species and ecosystems. The models are implemented in the R software  
635 environment with publicly accessible code. Testing at 10 streams in our study region indicated  
636 that models with seasonally variable flow effects had high prediction accuracy across all streams,  
637 suggesting that these models have broad applicability over a range of stream types. Our selected  
638 model, GAM7, incrementally improves upon previous methods for representing flow effects.  
639 Model applications include those explored here (i.e., scenario prediction and identifying periods  
640 of flow importance), as well as filling gaps in temperature time series. We suggest that GAM7,  
641 as well as similar model structures (i.e., GAM6, GAM8) will perform well across a range of  
642 streams. Model validation procedures, including extrapolation-based methods when models are  
643 applied to new data, should be conducted to test model accuracy at new sites and for datasets of  
644 variable periods of record.

645

#### 646 **CRedit authorship contribution statement**

647 J.E.A.: Conceptualization, Data curation, Methodology, Formal analysis, Visualization, Writing  
648 – original draft, Writing – review & editing. C.R.: Conceptualization, Investigation, Data  
649 curation, Funding acquisition, Project administration, Writing - review & editing. L.G.: Writing -  
650 review & editing.

651

#### 652 **Acknowledgments**

653 The Klamath Tribal Water Quality Consortium (Karuk Tribe, Yurok Tribe, Hoopa Valley Tribe,  
654 Quartz Valley Indian Reservation, and Resighini Rancheria) supported J.E.A. and L.G. using  
655 funds provided by the U.S. Environmental Protection Agency, Region 9. Maija Meneks (KNF)  
656 and Callie McConnell (USFS Corvallis) provided the USFS water temperature data. Isaiah  
657 Williams, Alex Case, Sean Ryan and Marla Bennett (QVIR) assisted with data collection. Taylor  
658 Daley (USFWS Arcata) provided USFWS water temperature data. Daniel Isaak and Sara John

659 provided data from Isaak et al. (2018) and FitzGerald et al. (2021), respectively. WRR editors  
660 and reviewers provided comments that substantially improved this manuscript.

661

## 662 **Data Availability Statement**

663 All input and output data and codes are archived in the online repository HydroShare (Asarian et  
664 al., 2023, <https://doi.org/10.4211/hs.a6653e2919964f9b840ec0340d86e11c>). USBR and USGS  
665 stream temperature data (Smith et al., 2018) are also available at [https://or.water.usgs.gov/cgi-](https://or.water.usgs.gov/cgi-bin/grapher/graph_setup.pl?site_id=11519500)  
666 [bin/grapher/graph\\_setup.pl?site\\_id=11519500](https://or.water.usgs.gov/cgi-bin/grapher/graph_setup.pl?site_id=11519500) and  
667 [https://cdec.water.ca.gov/dynamicapp/staMeta?station\\_id=RCL](https://cdec.water.ca.gov/dynamicapp/staMeta?station_id=RCL). CDWR stream temperature data  
668 are also available are available at  
669 <https://wdl.water.ca.gov/WaterDataLibrary/StationDetails.aspx?Station=F3410000>. Gridded  
670 PRISM air temperature data (Daly et al., 2008) are also available at:  
671 <https://prism.oregonstate.edu/explorer/>.

672

## 673 **References**

- 674 Alger, M., Lane, B. A., & Neilson, B. T. (2021). Combined influences of irrigation diversions  
675 and associated subsurface return flows on river temperature in a semi-arid region. *Hydrological*  
676 *Processes*, 35(8), e14283. <https://doi.org/10.1002/hyp.14283>
- 677 Amodio, S., Aria, M., & D'Ambrosio, A. (2014). On concurvity in nonlinear and nonparametric  
678 regression models. *Statistica*, 74(1), 85–98. <https://doi.org/10.6092/issn.1973-2201/4599>
- 679 Arismendi, I., Safeeq, M., Dunham, J. B., & Johnson, S. L. (2014). Can air temperature be used  
680 to project influences of climate change on stream temperature? *Environmental Research Letters*,  
681 9(8), 084015. <https://doi.org/10.1088/1748-9326/9/8/084015>
- 682 Arora, R., Tockner, K., & Venohr, M. (2016). Changing river temperatures in northern Germany:  
683 Trends and drivers of change. *Hydrological Processes*, 30(17), 3084–3096.  
684 <https://doi.org/10.1002/hyp.10849>
- 685 Asarian, J.E., Cressey, L., Bennett, B., Grunbaum, J., Cyr, L., Soto, T., & Robinson, C. (2020).  
686 Influence of snowpack, streamflow, air temperature, and wildfire smoke on Klamath Basin  
687 stream temperatures, 1995-2017. Eureka, CA: Riverbend Sciences.  
688 <https://doi.org/10.13140/RG.2.2.22934.47681>
- 689 Asarian, J. E., Robinson, C., & Genzoli, L. (2023). Data and codes for: Modeling seasonal  
690 effects of river flow on water temperatures in an agriculturally dominated California river  
691 [Dataset]. HydroShare, <https://doi.org/10.4211/hs.a6653e2919964f9b840ec0340d86e11c>
- 692 Asarian, J. E., & Walker, J. D. (2016). Long-term trends in streamflow and precipitation in  
693 Northwest California and Southwest Oregon, 1953-2012. *Journal of the American Water*  
694 *Resources Association*, 52(1), 241–261. <https://doi.org/10.1111/1752-1688.12381>
- 695 Baayen, R. H., van Rij, J., de Cat, C., & Wood, S. (2018). Autocorrelated errors in experimental  
696 data in the language sciences: some solutions offered by generalized additive mixed models. In  
697 D. Spielman, K. Heylen, & D. Geeraerts (Eds.), *Mixed-Effects Regression Models in Linguistics*  
698 (pp. 49–69). Springer International Publishing. [https://doi.org/10.1007/978-3-319-69830-4\\_4](https://doi.org/10.1007/978-3-319-69830-4_4)

- 699 Bartholow, J. M. (1991). A modeling assessment of the thermal regime for an urban sport  
700 fishery. *Environmental Management*, 15(6), 833. <https://doi.org/10.1007/BF02394821>
- 701 Benyahya, L., Caissie, D., St-Hilaire, A., Ouarda, T. B. M. J., & Bobée, B. (2007a). A review of  
702 statistical water temperature models. *Canadian Water Resources Journal / Revue Canadienne*  
703 *Des Ressources Hydriques*, 32(3), 179–192. <https://doi.org/10.4296/cwrj3203179>
- 704 Benyahya, L., St-Hilaire, A., Ouarda, T. B. M. J., Bobée, B., & Ahmadi-Nedushan, B. (2007b).  
705 Modeling of water temperatures based on stochastic approaches: Case study of the Deschutes  
706 River. *Journal of Environmental Engineering and Science*, 6(4), 437–448.  
707 <https://doi.org/10.1139/s06-067>
- 708 Benyahya, L., St-Hilaire, A., Ouarda, T., Bobee, B., & Dumas, J. (2008). Comparison of non-  
709 parametric and parametric water temperature models on the Nivelles River, France. *Hydrological*  
710 *Sciences Journal*, 53(3), 640–655.
- 711 Bogan, T., Mohseni, O., & Stefan, H. G. (2003). Stream temperature-equilibrium temperature  
712 relationship. *Water Resources Research*, 39(9), 1245. <https://doi.org/10.1029/2003WR002034>
- 713 Boudreault, J., Bergeron, N. E., St-Hilaire, A., & Chebana, F. (2019). Stream temperature  
714 modeling using functional regression models. *Journal of the American Water Resources*  
715 *Association*, 55(6), 1382–1400. <https://doi.org/10.1111/1752-1688.12778>
- 716 Boyd, M., and Kasper, B. (2003). Analytical methods for dynamic open channel heat and mass  
717 transfer: Methodology for Heat Source model version 7.0. Portland, OR: Oregon Department of  
718 Environmental Quality.
- 719 Brewitt, K. S., & Danner, E. M. (2014). Spatio-temporal temperature variation influences  
720 juvenile steelhead (*Oncorhynchus mykiss*) use of thermal refuges. *Ecosphere*, 5(7), art92.  
721 <https://doi.org/10.1890/ES14-00036.1>
- 722 Briggs, M. A., Johnson, Z. C., Snyder, C. D., Hitt, N. P., Kurylyk, B. L., Lautz, L., Irvine, D. J.,  
723 Hurley, S. T., & Lane, J. W. (2018). Inferring watershed hydraulics and cold-water habitat  
724 persistence using multi-year air and stream temperature signals. *Science of The Total*  
725 *Environment*, 636, 1117–1127. <https://doi.org/10.1016/j.scitotenv.2018.04.344>
- 726 Brown, G. W. (1969). Predicting temperatures of small streams. *Water Resources Research*,  
727 5(1), 68–75. <https://doi.org/10.1029/WR005i001p00068>
- 728 Cade, B. S., & Noon, B. R. (2003). A gentle introduction to quantile regression for ecologists.  
729 *Frontiers in Ecology and the Environment*, 1(8), 412–420. [https://doi.org/10.1890/1540-9295\(2003\)001\[0412:AGITQR\]2.0.CO;2](https://doi.org/10.1890/1540-9295(2003)001[0412:AGITQR]2.0.CO;2)
- 731 Caissie, D. (2006). The thermal regime of rivers: A review. *Freshwater Biology*, 51(8), 1389–  
732 1406. <https://doi.org/10.1111/j.1365-2427.2006.01597.x>
- 733 Caissie, D., El-Jabi, N., & Satish, M. G. (2001). Modelling of maximum daily water  
734 temperatures in a small stream using air temperatures. *Journal of Hydrology*, 251(1), 14–28.  
735 [https://doi.org/10.1016/S0022-1694\(01\)00427-9](https://doi.org/10.1016/S0022-1694(01)00427-9)
- 736 Caldwell, R. J., Gangopadhyay, S., Bountry, J., Lai, Y., & Elsner, M. M. (2013). Statistical  
737 modeling of daily and subdaily stream temperatures: Application to the Methow River Basin,  
738 Washington. *Water Resources Research*, 49(7), 4346–4361. <https://doi.org/10.1002/wrcr.20353>

- 739 CDFW (California Department of Fish and Wildlife) (2017). Interim Instream Flow Criteria for  
740 the Protection of Fishery Resources in the Scott River Watershed, Siskiyou County.  
741 [https://web.archive.org/web/20210324204650if\\_/https://nrm.dfg.ca.gov/FileHandler.ashx?Docu](https://web.archive.org/web/20210324204650if_/https://nrm.dfg.ca.gov/FileHandler.ashx?DocumentID=143476)  
742 [mentID=143476](https://web.archive.org/web/20210324204650if_/https://nrm.dfg.ca.gov/FileHandler.ashx?DocumentID=143476).
- 743 Chandesaris, A., Van Looy, K., Diamond, J. S., & Souchon, Y. (2019). Small dams alter thermal  
744 regimes of downstream water. *Hydrology and Earth System Sciences*, 23(11), 4509–4525.  
745 <https://doi.org/10.5194/hess-23-4509-2019>
- 746 Cline, T. J., Schindler, D. E., Walsworth, T. E., French, D. W., & Lisi, P. J. (2020). Low  
747 snowpack reduces thermal response diversity among streams across a landscape. *Limnology and*  
748 *Oceanography Letters*, 5(3), 254–263. <https://doi.org/10.1002/lol2.10148>.
- 749 Coleman, D., Bevitt, R., & Reinfelds, I. (2021). Predicting the thermal regime change of a  
750 regulated snowmelt river using a generalised additive model and analogue reference streams.  
751 *Environmental Processes*, 8(2), 511–531. <https://doi.org/10.1007/s40710-021-00501-7>
- 752 Crozier, L. G., Siegel, J. E., Wiesebron, L. E., Trujillo, E. M., Burke, B. J., Sandford, B. P., &  
753 Widener, D. L. (2020). Snake River sockeye and Chinook salmon in a changing climate:  
754 Implications for upstream migration survival during recent extreme and future climates. *PLOS*  
755 *ONE*, 15(9), e0238886. <https://doi.org/10.1371/journal.pone.0238886>
- 756 Dahlke, H., Brown, A., Orloff, S., Putnam, D., & O’Geen, T. (2018). Managed winter flooding  
757 of alfalfa recharges groundwater with minimal crop damage. *California Agriculture*, 72(1), 1–11.  
758 <https://doi.org/10.3733/ca.2018a0001>
- 759 Daly, C., Halbleib, M., Smith, J. I., Gibson, W. P., Doggett, M. K., Taylor, G. H., Curtis, J., &  
760 Pasteris, P. P. (2008). Physiographically sensitive mapping of climatological temperature and  
761 precipitation across the conterminous United States. *International Journal of Climatology*,  
762 28(15), 2031–2064. <https://doi.org/10.1002/joc.1688>
- 763 David, A. T., Asarian, J. E., & Lake, F. K. (2018). Wildfire smoke cools summer river and  
764 stream water temperatures. *Water Resources Research*, 54(10), 7273–7290.  
765 <https://doi.org/10.1029/2018WR022964>
- 766 Drake, D., Tate, K., & Carlson, H. (2000). Analysis shows climate-caused decreases in Scott  
767 River fall flows. *California Agriculture*, 54(6), 46–49. <https://doi.org/10.3733/ca.v054n06p46>
- 768 Dugdale, S. J., Hannah, D. M., & Malcolm, I. A. (2017). River temperature modelling: A review  
769 of process-based approaches and future directions. *Earth-Science Reviews*, 175, 97–113.  
770 <https://doi.org/10.1016/j.earscirev.2017.10.009>
- 771 Dugdale, S. J., Malcolm, I. A., Kantola, K., & Hannah, D. M. (2018). Stream temperature under  
772 contrasting riparian forest cover: Understanding thermal dynamics and heat exchange processes.  
773 *Science of The Total Environment*, 610–611, 1375–1389.  
774 <https://doi.org/10.1016/j.scitotenv.2017.08.198>
- 775 Dunham, J., Chandler, G., Rieman, B., Martin, D. (2005). Measuring stream temperature with  
776 digital data loggers: A user’s guide (*USDA Forest Service Gen. Tech. Rep. RMRS-GTR-*  
777 *150WWW*). [http://www.fs.fed.us/rm/pubs/rmrs\\_gtr150.pdf](http://www.fs.fed.us/rm/pubs/rmrs_gtr150.pdf)
- 778 Dymond, J. R. (1984). Water temperature change caused by abstraction. *Journal of Hydraulic*  
779 *Engineering*, 110(7), 987–991. [https://doi.org/10.1061/\(ASCE\)0733-9429\(1984\)110:7\(987\)](https://doi.org/10.1061/(ASCE)0733-9429(1984)110:7(987))

- 780 Fasiolo, M., Wood, S. N., Zaffran, M., Nedellec, R., & Goude, Y. (2020). Fast calibrated  
781 additive quantile regression. *Journal of the American Statistical Association*, 1–11.  
782 <https://doi.org/10.1080/01621459.2020.1725521>
- 783 Ficklin, D. L., Barnhart, B. L., Knouft, J. H., Stewart, I. T., Maurer, E. P., Letsinger, S. L., &  
784 Whittaker, G. W. (2014). Climate change and stream temperature projections in the Columbia  
785 River basin: Habitat implications of spatial variation in hydrologic drivers. *Hydrology and Earth  
786 System Sciences*, 18(12), 4897–4912. <https://doi.org/10.5194/hess-18-4897-2014>
- 787 FitzGerald, A. M., John, S. N., Apgar, T. M., Mantua, N. J., & Martin, B. T. (2021). Quantifying  
788 thermal exposure for migratory riverine species: Phenology of Chinook salmon populations  
789 predicts thermal stress. *Global Change Biology*, 27(3), 536–549.  
790 <https://doi.org/10.1111/gcb.15450>
- 791 Foglia, L., McNally, A., & Harter, T. (2013). Coupling a spatiotemporally distributed soil water  
792 budget with stream-depletion functions to inform stakeholder-driven management of  
793 groundwater-dependent ecosystems. *Water Resources Research*, 49(11), 7292–7310.  
794 <https://doi.org/10.1002/wrcr.20555>
- 795 Foglia, L., Neumann, J., Tolley, D., Orloff, S., Snyder, R., & Harter, T. (2018). Modeling guides  
796 groundwater management in a basin with river–aquifer interactions. *California Agriculture*,  
797 72(1), 84–95. <https://doi.org/10.3733/ca.2018a0011>
- 798 Folegot, S., Hannah, D. M., Dugdale, S. J., Kurz, M. J., Drummond, J. D., Klaar, M. J., Lee-  
799 Cullin, J., Keller, T., Martí, E., Zarnetske, J. P., Ward, A. S., & Krause, S. (2018). Low flow  
800 controls on stream thermal dynamics. *Limnologia*, 68, 157–167.  
801 <https://doi.org/10.1016/j.limno.2017.08.003>
- 802 Fullerton, A. H., Torgersen, C. E., Lawler, J. J., Faux, R. N., Steel, E. A., Beechie, T. J.,  
803 Ebersole, J. L., & Leibowitz, S. G. (2015). Rethinking the longitudinal stream temperature  
804 paradigm: Region-wide comparison of thermal infrared imagery reveals unexpected complexity  
805 of river temperatures. *Hydrological Processes*, 29(22), 4719–4737.  
806 <https://doi.org/10.1002/hyp.10506>
- 807 Gibeau, P., & Palen, W. J. (2020). Predicted effects of flow diversion by run-of-river  
808 hydropower on bypassed stream temperature and bioenergetics of salmonid fishes. *River  
809 Research and Applications*, 36(9), 1903–1915. <https://doi.org/10.1002/rra.3706>
- 810 Georges, B., Michez, A., Latte, N., Lejeune, P., & Brostaux, Y. (2021). Water stream heating  
811 dynamics around extreme temperature events: An innovative method combining GAM and  
812 differential equations. *Journal of Hydrology*, 601, 126600.  
813 <https://doi.org/10.1016/j.jhydrol.2021.126600>
- 814 Glover, R. S., Soulsby, C., Fryer, R. J., Birkel, C., & Malcolm, I. A. (2020). Quantifying the  
815 relative importance of stock level, river temperature and discharge on the abundance of juvenile  
816 Atlantic salmon (*Salmo salar*). *Ecohydrology*, 13(6), e2231. <https://doi.org/10.1002/eco.2231>
- 817 Gu, R. R., & Li, Y. (2002). River temperature sensitivity to hydraulic and meteorological  
818 parameters. *Journal of Environmental Management*, 66(1), 43–56.  
819 <https://doi.org/10.1006/jema.2002.0565>

- 820 Gu, R., Montgomery, S., & Austin, T. A. (1998). Quantifying the effects of stream discharge on  
821 summer river temperature. *Hydrological Sciences Journal*, 43(6), 885–904.  
822 <https://doi.org/10.1080/02626669809492185>
- 823 Hannah, D. M., Malcolm, I. A., & Bradley, C. (2009). Seasonal hyporheic temperature dynamics  
824 over riffle bedforms. *Hydrological Processes*, 23(15), 2178–2194.  
825 <https://doi.org/10.1002/hyp.7256>
- 826 Imholt, C., Gibbins, C. N., Malcolm, I. A., Langan, S., & Soulsby, C. (2010). Influence of  
827 riparian cover on stream temperatures and the growth of the mayfly *Baetis rhodani* in an upland  
828 stream. *Aquatic Ecology*, 44(4), 669–678. <https://doi.org/10.1007/s10452-009-9305-0>
- 829 Isaak, D. J., Luce, C. H., Horan, D. L., Chandler, G. L., Wollrab, S. P., Dubois, W. B., & Nagel,  
830 D. E. (2020). Thermal regimes of perennial rivers and streams in the Western United States.  
831 *Journal of the American Water Resources Association*, 1752-1688.12864.  
832 <https://doi.org/10.1111/1752-1688.12864>
- 833 Isaak, D. J., Luce, C. H., Horan, D. L., Chandler, G. L., Wollrab, S. P., & Nagel, D. E. (2018).  
834 Global warming of salmon and trout rivers in the Northwestern U.S.: Road to ruin or path  
835 through purgatory? *Transactions of the American Fisheries Society*, 147(3), 566–587.  
836 <https://doi.org/10.1002/tafs.10059>
- 837 Isaak, D. J., Wenger, S. J., Peterson, E. E., Hoef, J. M. V., Nagel, D. E., Luce, C. H., Hostetler,  
838 S. W., Dunham, J. B., Roper, B. B., Wollrab, S. P., Chandler, G. L., Horan, D. L., & Parkes-  
839 Payne, S. (2017). The NorWeST summer stream temperature model and scenarios for the  
840 Western U.S.: A crowd-sourced database and new geospatial tools foster a user community and  
841 predict broad climate warming of rivers and streams. *Water Resources Research*, 53(11), 9181–  
842 9205. <https://doi.org/10.1002/2017WR020969>
- 843 Islam, S. U., Hay, R. W., Déry, S. J., & Booth, B. P. (2019). Modelling the impacts of climate  
844 change on riverine thermal regimes in western Canada’s largest Pacific watershed. *Scientific*  
845 *Reports*, 9, 11398. <https://doi.org/10.1038/s41598-019-47804-2>
- 846 Jackson, F. L., Fryer, R. J., Hannah, D. M., Millar, C. P., & Malcolm, I. A. (2018). A spatio-  
847 temporal statistical model of maximum daily river temperatures to inform the management of  
848 Scotland’s Atlantic salmon rivers under climate change. *Science of The Total Environment*, 612,  
849 1543–1558. <https://doi.org/10.1016/j.scitotenv.2017.09.010>
- 850 Johnson, S. L. (2004). Factors influencing stream temperatures in small streams: Substrate  
851 effects and a shading experiment. *Canadian Journal of Fisheries and Aquatic Sciences*, 61(6),  
852 913–923.
- 853 Johnson, Z. C., Johnson, B. G., Briggs, M. A., Snyder, C. D., Hitt, N. P., & Devine, W. D.  
854 (2021). Heed the data gap: Guidelines for using incomplete datasets in annual stream  
855 temperature analyses. *Ecological Indicators*, 122, 107229.  
856 <https://doi.org/10.1016/j.ecolind.2020.107229>
- 857 Kelleher, C., Wagener, T., Gooseff, M., McGlynn, B., McGuire, K., & Marshall, L. (2012).  
858 Investigating controls on the thermal sensitivity of Pennsylvania streams. *Hydrological*  
859 *Processes*, 26(5), 771–785. <https://doi.org/10.1002/hyp.8186>

- 860 Kim, J.-S., & Jain, S. (2010). High-resolution streamflow trend analysis applicable to annual  
861 decision calendars: A western United States case study. *Climatic Change*, 102(3–4), 699–707.  
862 <https://doi.org/10.1007/s10584-010-9933-3>
- 863 KNF (Klamath National Forest) (2010). Klamath National Forest Sediment and Temperature  
864 Monitoring Plan and Quality Assurance Project Plan. Yreka, CA: Klamath National Forest.  
865 [https://web.archive.org/web/http://www.waterboards.ca.gov/water\\_issues/programs/tmdl/records](https://web.archive.org/web/http://www.waterboards.ca.gov/water_issues/programs/tmdl/records/region_1/2013/ref4082.pdf)  
866 [/region\\_1/2013/ref4082.pdf](https://web.archive.org/web/http://www.waterboards.ca.gov/water_issues/programs/tmdl/records/region_1/2013/ref4082.pdf).
- 867 KNF (Klamath National Forest) (2011). Klamath National Forest, Water and Air Temperature  
868 Monitoring Protocol, May 2011. Yreka, CA: Klamath National Forest.
- 869 Klemeš, V. (1986). Operational testing of hydrological simulation models. *Hydrological*  
870 *Sciences Journal*, 31(1), 13–24. <https://doi.org/10.1080/02626668609491024>
- 871 Klos, P. Z., Link, T. E., & Abatzoglou, J. T. (2014). Extent of the rain-snow transition zone in  
872 the western U.S. under historic and projected climate. *Geophysical Research Letters*, 41(13),  
873 4560–4568. <https://doi.org/10.1002/2014GL060500>
- 874 Koch, H., & Grünwald, U. (2010). Regression models for daily stream temperature simulation:  
875 Case studies for the river Elbe, Germany. *Hydrological Processes*, 24(26), 3826–3836.  
876 <https://doi.org/10.1002/hyp.7814>
- 877 Kurylyk, B. L., MacQuarrie, K. T. B., Linnansaari, T., Cunjak, R. A., & Curry, R. A. (2015).  
878 Preserving, augmenting, and creating cold-water thermal refugia in rivers: Concepts derived  
879 from research on the Miramichi River, New Brunswick (Canada). *Ecohydrology*, 8(6), 1095–  
880 1108. <https://doi.org/10.1002/eco.1566>
- 881 Laanaya, F., St-Hilaire, A., & Gloaguen, E. (2017). Water temperature modelling: Comparison  
882 between the generalized additive model, logistic, residuals regression and linear regression  
883 models. *Hydrological Sciences Journal*, 62(7), 1078–1093.  
884 <https://doi.org/10.1080/02626667.2016.1246799>
- 885 Leach, J. A., & Moore, R. D. (2019). Empirical stream thermal sensitivities may underestimate  
886 stream temperature response to climate warming. *Water Resources Research*, 55(7), 5453–5467.  
887 <https://doi.org/10.1029/2018WR024236>
- 888 Lee, S.-Y., Fullerton, A. H., Sun, N., & Torgersen, C. E. (2020). Projecting spatiotemporally  
889 explicit effects of climate change on stream temperature: A model comparison and implications  
890 for coldwater fishes. *Journal of Hydrology*, 588, 125066.  
891 <https://doi.org/10.1016/j.jhydrol.2020.125066>
- 892 Letcher, B. H., Hocking, D. J., O’Neil, K., Whiteley, A. R., Nislow, K. H., & O’Donnell, M. J.  
893 (2016). A hierarchical model of daily stream temperature using air-water temperature  
894 synchronization, autocorrelation, and time lags. *PeerJ*, 4, e1727.  
895 <https://doi.org/10.7717/peerj.1727>
- 896 Li, H., Deng, X., Kim, D.-Y., & Smith, E. P. (2014). Modeling maximum daily temperature  
897 using a varying coefficient regression model. *Water Resources Research*, 50(4), 3073–3087.  
898 <https://doi.org/10.1002/2013WR014243>

- 899 Luce, C., Staab, B., Kramer, M., Wenger, S., Isaak, D., & McConnell, C. (2014). Sensitivity of  
900 summer stream temperatures to climate variability in the Pacific Northwest. *Water Resources*  
901 *Research*, 50(4), 3428–3443. <https://doi.org/10.1002/2013WR014329>
- 902 Luo, Y., Ficklin, D. L., Liu, X., & Zhang, M. (2013). Assessment of climate change impacts on  
903 hydrology and water quality with a watershed modeling approach. *Science of The Total*  
904 *Environment*, 450–451, 72–82. <https://doi.org/10.1016/j.scitotenv.2013.02.004>
- 905 Lute, A. C., & Luce, C. H. (2017). Are model transferability and complexity antithetical?  
906 Insights from validation of a variable-complexity empirical snow model in space and time. *Water*  
907 *Resources Research*, 53(11), 8825–8850. <https://doi.org/10.1002/2017WR020752>
- 908 Manhard, C. V., N. A. Som, E. C. Jones, & R. W. Perry. 2018. Estimation of stream conditions  
909 in tributaries of the Klamath River, Northern California (*Arcata Fisheries Technical Report*  
910 Number TR 2018-32). Arcata, CA: U.S. Fish and Wildlife Service.  
911 [https://web.archive.org/web/https://www.fws.gov/arcata/fisheries/reports/technical/2018/Estimati](https://web.archive.org/web/https://www.fws.gov/arcata/fisheries/reports/technical/2018/EstimationofStreamConditionsinTributariesoftheKlamathRiverNorthernCalifornia.pdf)  
912 [onofStreamConditionsinTributariesoftheKlamathRiverNorthernCalifornia.pdf](https://web.archive.org/web/https://www.fws.gov/arcata/fisheries/reports/technical/2018/EstimationofStreamConditionsinTributariesoftheKlamathRiverNorthernCalifornia.pdf)
- 913 Mayer, T. D. (2012). Controls of summer stream temperature in the Pacific Northwest. *Journal*  
914 *of Hydrology*, 475(0), 323–335. <https://doi.org/10.1016/j.jhydrol.2012.10.012>
- 915 Meier, W., Bonjour, C., Wüest, A., & Reichert, P. (2003). Modeling the effect of water diversion  
916 on the temperature of mountain streams. *Journal of Environmental Engineering*, 129(8), 755–  
917 764. [https://doi.org/10.1061/\(ASCE\)0733-9372\(2003\)129:8\(755\)](https://doi.org/10.1061/(ASCE)0733-9372(2003)129:8(755))
- 918 Mierau, D. W., Trush, W. J., Rossi, G. J., Carah, J. K., Clifford, M. O., & Howard, J. K. (2017).  
919 Managing diversions in unregulated streams using a modified percent-of-flow approach.  
920 *Freshwater Biology*. <https://doi.org/10.1111/fwb.12985>
- 921 Mohseni, O., & Stefan, H. G. (1999). Stream temperature/air temperature relationship: A  
922 physical interpretation. *Journal of Hydrology*, 218(3), 128–141. [https://doi.org/10.1016/S0022-](https://doi.org/10.1016/S0022-1694(99)00034-7)  
923 [1694\(99\)00034-7](https://doi.org/10.1016/S0022-1694(99)00034-7)
- 924 Mohseni, O., Stefan, H. G., & Erickson, T. R. (1998). A nonlinear regression model for weekly  
925 stream temperatures. *Water Resources Research*, 34(10), 2685–2692.  
926 <https://doi.org/10.1029/98WR01877>
- 927 Moore, R. D., Spittlehouse, D. L., & Story, A. (2005). Riparian microclimate and stream  
928 temperature response to forest harvesting: A review. *Journal of the American Water Resources*  
929 *Association*, 41(4), 813–834. <https://doi.org/10.1111/j.1752-1688.2005.tb03772.x>
- 930 Neumann David W., Rajagopalan Balaji, & Zagona Edith A. (2003). Regression model for daily  
931 maximum stream temperature. *Journal of Environmental Engineering*, 129(7), 667–674.  
932 [https://doi.org/10.1061/\(ASCE\)0733-9372\(2003\)129:7\(667\)](https://doi.org/10.1061/(ASCE)0733-9372(2003)129:7(667))
- 933 Nichols, A. L., Willis, A. D., Jeffres, C. A., & Deas, M. L. (2014). Water temperature patterns  
934 below large groundwater springs: management implications for coho salmon in the Shasta River,  
935 California. *River Research and Applications*, 30(4), 442–455. <https://doi.org/10.1002/rra.2655>
- 936 NCRWQCB (North Coast Regional Water Quality Control Board) (2005). *Staff Report for the*  
937 *Action Plan for the Scott River Watershed Sediment and Temperature Total Maximum Daily*  
938 *Loads*. Santa Rosa, CA: North Coast Regional Water Quality Control Board.  
939 [https://www.waterboards.ca.gov/northcoast/water\\_issues/programs/tmdls/scott\\_river/staff\\_report](https://www.waterboards.ca.gov/northcoast/water_issues/programs/tmdls/scott_river/staff_report)

- 940 Null, S. E., Mouzon, N. R., & Elmore, L. R. (2017). Dissolved oxygen, stream temperature, and  
941 fish habitat response to environmental water purchases. *Journal of Environmental Management*,  
942 197, 559–570. <https://doi.org/10.1016/j.jenvman.2017.04.016>
- 943 Null, S. E., Viers, J. H., Deas, M. L., Tanaka, S. K., & Mount, J. F. (2013). Stream temperature  
944 sensitivity to climate warming in California's Sierra Nevada: Impacts to coldwater habitat.  
945 *Climatic Change*, 116(1), 149–170. <https://doi.org/10.1007/s10584-012-0459-8>
- 946 Ouellet, V., St-Hilaire, A., Dugdale, S. J., Hannah, D. M., Krause, S., & Proulx-Ouellet, S.  
947 (2020). River temperature research and practice: Recent challenges and emerging opportunities  
948 for managing thermal habitat conditions in stream ecosystems. *Science of The Total*  
949 *Environment*, 736, 139679. <https://doi.org/10.1016/j.scitotenv.2020.139679>
- 950 Pedersen, E. J., Miller, D. L., Simpson, G. L., & Ross, N. (2019). Hierarchical generalized  
951 additive models in ecology: An introduction with mgcv. *PeerJ*, 7, e6876.  
952 <https://doi.org/10.7717/peerj.6876>
- 953 Persad, G. G., Swain, D. L., Kouba, C., & Ortiz-Partida, J. P. (2020). Inter-model agreement on  
954 projected shifts in California hydroclimate characteristics critical to water management. *Climatic*  
955 *Change*. <https://doi.org/10.1007/s10584-020-02882-4>
- 956 Piotrowski, A. P., & Napiorkowski, J. J. (2019). Simple modifications of the nonlinear  
957 regression stream temperature model for daily data. *Journal of Hydrology*, 572, 308–328.  
958 <https://doi.org/10.1016/j.jhydrol.2019.02.035>
- 959 Poff, N. L., Tharme, R. E., & Arthington, A. H. (2017). Evolution of environmental flows  
960 assessment science, principles, and methodologies. In A. C. Horne, J. A. Webb, M. J.  
961 Stewardson, B. Richter, & M. Acreman (Eds.), *Water for the Environment* (pp. 203–236).  
962 Academic Press. <https://doi.org/10.1016/B978-0-12-803907-6.00011-5>
- 963 QVIR (Quartz Valley Indian Reservation) (2016). Quality assurance project plan 2016 revision  
964 water quality sampling and analysis, CWA 106 grant identification # I-96927206-0. Fort Jones,  
965 CA: QVIR Tribal Environmental Protection Department.
- 966 Railsback, S. F., Harvey, B. C., Kupferberg, S. J., Lang, M. M., McBain, S., & Welsh, H. H.  
967 (2016). Modeling potential river management conflicts between frogs and salmonids. *Canadian*  
968 *Journal of Fisheries and Aquatic Sciences*, 73(5), 773–784. <https://doi.org/10.1139/cjfas-2015-0267>
- 970 Roberts, D. R., Bahn, V., Ciuti, S., Boyce, M. S., Elith, J., Guillera-Arroita, G., Hauenstein, S.,  
971 Lahoz-Monfort, J. J., Schröder, B., Thuiller, W., Warton, D. I., Wintle, B. A., Hartig, F., &  
972 Dormann, C. F. (2017). Cross-validation strategies for data with temporal, spatial, hierarchical,  
973 or phylogenetic structure. *Ecography*, 40(8), 913–929. <https://doi.org/10.1111/ecog.02881>
- 974 Romberger, C. Z. and S. Gwozdz (2018). Performance of water temperature management on the  
975 Klamath and Trinity Rivers, 2017. (*U.S. Fish and Wildlife Service, Arcata Fisheries Data Series*  
976 *Number DS 2018-59*).
- 977 Santiago, J. M., Muñoz-Mas, R., Solana-Gutiérrez, J., García de Jalón, D., Alonso, C., Martínez-  
978 Capel, F., Pórtoles, J., Monjo, R., & Ribalaygua, J. (2017). Waning habitats due to climate  
979 change: The effects of changes in streamflow and temperature at the rear edge of the distribution  
980 of a cold-water fish. *Hydrology and Earth System Sciences*, 21(8), 4073–4101.  
981 <https://doi.org/10.5194/hess-21-4073-2017>

- 982 Shaw, S. B. (2017). Does an upper limit to river water temperature apply in all places?  
983 *Hydrological Processes*, 31(21), 3729–3739. <https://doi.org/10.1002/hyp.11297>
- 984 Siegel, J. E., & Volk, C. J. (2019). Accurate spatiotemporal predictions of daily stream  
985 temperature from statistical models accounting for interactions between climate and landscape.  
986 *PeerJ*, 7, e7892. <https://doi.org/10.7717/peerj.7892>
- 987 Sinokrot, B. A., & Gulliver, J. S. (2000). In-stream flow impact on river water temperatures.  
988 *Journal of Hydraulic Research*, 38(5), 339–349. <https://doi.org/10.1080/00221680009498315>
- 989 Sohrabi, M. M., Benjankar, R., Tonina, D., Wenger, S. J., & Isaak, D. J. (2017). Estimation of  
990 daily stream water temperatures with a Bayesian regression approach. *Hydrological Processes*,  
991 31(9), 1719–1733. <https://doi.org/10.1002/hyp.11139>
- 992 Smith, C. D., Rounds, S. A., & Orzol, L. L. (2018). Klamath River Basin water-quality data.  
993 (USGS Numbered Series *Fact Sheet* 2018–3031). <https://doi.org/10.3133/fs20183031>
- 994 Soto, B. (2016). Assessment of Trends in Stream Temperatures in the North of the Iberian  
995 Peninsula Using a Nonlinear Regression Model for the Period 1950–2013. *River Research and*  
996 *Applications*, 32(6), 1355–1364. <https://doi.org/10.1002/rra.2971>
- 997 Stanford, J.A. & Ward, J.V. (1992). Management of aquatic resources in large catchments:  
998 Recognizing interactions between ecosystem connectivity and environmental disturbance. In R.  
999 J. Naiman (Editor). *Watershed Management: Balancing Sustainability and Environmental*  
1000 *Change* (pp. 91–124). New York, NY: Springer.
- 1001 Siegel, J. E., Fullerton, A. H., & Jordan, C. E. (2022). Accounting for snowpack and time-  
1002 varying lags in statistical models of stream temperature. *Journal of Hydrology X*, 17, 100136.  
1003 <https://doi.org/10.1016/j.hydroa.2022.100136>
- 1004 St-Hilaire, A., Boyer, C., Bergeron, N., & Daigle, A. (2018). Water temperature monitoring in  
1005 Eastern Canada: A case study for network optimization. *WIT Transactions on Ecology and the*  
1006 *Environment*, 228, 269–275. <https://doi.org/10.2495/WP180251>
- 1007 Steel, E. A., Beechie, T. J., Torgersen, C. E., & Fullerton, A. H. (2017). Envisioning,  
1008 quantifying, and managing thermal regimes on river networks. *BioScience*, 67(6), 506–522.  
1009 <https://doi.org/10.1093/biosci/bix047>
- 1010 Superior Court of Siskiyou County (1980). Scott River adjudication, decree no. 30662. Scott  
1011 River stream system, Siskiyou County. Sacramento, CA: State Water Resources Control Board.
- 1012 Sutton, R. J., Deas, M. L., Tanaka, S. K., Soto, T., & Corum, R. A. (2007). Salmonid  
1013 observations at a Klamath River thermal refuge under various hydrological and meteorological  
1014 conditions. *River Research and Applications*, 23(7), 775–785.
- 1015 Sutton, R., & Soto, T. (2012). Juvenile coho salmon behavioural characteristics in Klamath river  
1016 summer thermal refugia. *River Research and Applications*. <https://doi.org/10.1002/rra.1459>
- 1017 Tague, C., Farrell, M., Grant, G., Lewis, S., & Rey, S. (2007). Hydrogeologic controls on  
1018 summer stream temperatures in the McKenzie River basin, Oregon. *Hydrological Processes*,  
1019 21(24), 3288–3300. <https://doi.org/10.1002/hyp.6538>
- 1020 Theurer, F.D., Voos, K.A., & Miller, W.J. (1984). Instream water temperature model. *Instream*  
1021 *Flow Information Paper 16*. FWS/OBS-84/15. Washington, D.C.: US Fish and Wildlife Service.

- 1022 Tolley, D., Foglia, L., & Harter, T. (2019). Sensitivity analysis and calibration of an integrated  
1023 hydrologic model in an irrigated agricultural basin with a groundwater-dependent ecosystem.  
1024 *Water Resources Research*, 55(9), 7876–7901. <https://doi.org/10.1029/2018WR024209>
- 1025 USEPA (U.S. Environmental Protection Agency) (2003). EPA Region 10 guidance for Pacific  
1026 Northwest state and tribal temperature water quality standards. EPA 910-B-03-002. Seattle, WA:  
1027 Region 10 Office of Water.
- 1028 Van Kirk, R. W., & Naman, S. W. (2008). Relative effects of climate and water use on base-flow  
1029 trends in the Lower Klamath Basin. *Journal of the American Water Resources Association*,  
1030 44(4), 1035–1052. <https://doi.org/10.1111/j.1752-1688.2008.00212.x>
- 1031 VanderKooi, S., Thorsteinson, L., & Clark, M. (2011). Environmental and historical setting. In  
1032 L. Thorsteinson, S. VanderKooi, & W. Duffy (Eds.), *Proceedings of the Klamath Basin Science*  
1033 *Conference*, Medford, Oregon, February 1–5, 2010 (pp. 31–36). Reston, VA: U.S. Geological  
1034 Survey.
- 1035 van Rij, J., Hendriks, P., van Rijn, H., Baayen, R. H., & Wood, S. N. (2019). Analyzing the time  
1036 course of pupillometric data. *Trends in Hearing*, 23, 233121651983248.  
1037 <https://doi.org/10.1177/2331216519832483>
- 1038 van Rij, J., Wieling, M., Baayen, R., van Rijn, H. (2020). itsadug: Interpreting time series and  
1039 autocorrelated data using GAMMs. *R package version 2.4*. [https://cran.r-](https://cran.r-project.org/package=itsadug)  
1040 [project.org/package=itsadug](https://cran.r-project.org/package=itsadug)
- 1041 van Vliet, M. T. H., Ludwig, F., Zwolsman, J. J. G., Weedon, G. P., & Kabat, P. (2011). Global  
1042 river temperatures and sensitivity to atmospheric warming and changes in river flow. *Water*  
1043 *Resources Research*, 47(2). <https://doi.org/10.1029/2010WR009198>
- 1044 Webb, B. W., Clack, P. D., & Walling, D. E. (2003). Water–air temperature relationships in a  
1045 Devon river system and the role of flow. *Hydrological Processes*, 17(15), 3069–3084.  
1046 <https://doi.org/10.1002/hyp.1280>
- 1047 Webb, B. W., Hannah, D. M., Moore, R. D., Brown, L. E., & Nobilis, F. (2008). Recent  
1048 advances in stream and river temperature research. *Hydrological Processes*, 22(7), 902–918.  
1049 <https://doi.org/10.1002/hyp.6994>
- 1050 Wenger, S. J., Isaak, D. J., Luce, C. H., Neville, H. M., Fausch, K. D., Dunham, J. B., Dauwalter,  
1051 D. C., Young, M. K., Elsner, M. M., Rieman, B. E., Hamlet, A. F., & Williams, J. E. (2011).  
1052 Flow regime, temperature, and biotic interactions drive differential declines of trout species  
1053 under climate change. *Proceedings of the National Academy of Sciences*, 108(34), 14175–14180.  
1054 <https://doi.org/10.1073/pnas.1103097108>
- 1055 Westerling, A. L. (2016). Increasing western US forest wildfire activity: Sensitivity to changes in  
1056 the timing of spring. *Philosophical Transactions of the Royal Society B: Biological Sciences*,  
1057 371(1696), 20150178. <https://doi.org/10.1098/rstb.2015.0178>
- 1058 Wood, S.N. (2017). *Generalized additive models: An introduction with R (2nd edition)*.  
1059 Chapman and Hall/CRC.
- 1060 Wrzesiński, D., & Graf, R. (2022). Temporal and spatial patterns of the river flow and water  
1061 temperature relations in Poland. *Journal of Hydrology and Hydromechanics*, 70(1), 12–29.  
1062 <https://doi.org/10.2478/johh-2021-0033>

- 1063 Yan, H., Sun, N., Fullerton, A., & Baerwalde, M. (2021). Greater vulnerability of snowmelt-fed  
1064 river thermal regimes to a warming climate. *Environmental Research Letters*, 16(5), 054006.  
1065 <https://doi.org/10.1088/1748-9326/abf393>
- 1066 Yang, G., & Moyer, D. L. (2020). Estimation of nonlinear water-quality trends in high-frequency  
1067 monitoring data. *Science of The Total Environment*, 715, 136686.  
1068 <https://doi.org/10.1016/j.scitotenv.2020.136686>
- 1069 Yard, M. D., Bennett, G. E., Mietz, S. N., Coggins, L. G., Stevens, L. E., Hueftle, S., & Blinn, D.  
1070 W. (2005). Influence of topographic complexity on solar insolation estimates for the Colorado  
1071 River, Grand Canyon, AZ. *Ecological Modelling*, 183(2), 157–172.  
1072 <https://doi.org/10.1016/j.ecolmodel.2004.07.027>
- 1073 Yarnell, S. M., Stein, E. D., Webb, J. A., Grantham, T., Lusardi, R. A., Zimmerman, J., Peek, R.  
1074 A., Lane, B. A., Howard, J., & Sandoval-Solis, S. (2020). A functional flows approach to  
1075 selecting ecologically relevant flow metrics for environmental flow applications. *River Research*  
1076 *and Applications*, rra.3575. <https://doi.org/10.1002/rra.3575>

1077

#### 1078 **References From the Supporting Information**

- 1079 Daly, C., Doggett, M. K., Smith, J. I., Olson, K. V., Halbleib, M. D., Dimcovic, Z., Keon, D.,  
1080 Loiselle, R. A., Steinberg, B., Ryan, A. D., Pancake, C. M., & Kaspar, E. M. (2021). Challenges  
1081 in observation-based mapping of daily precipitation across the conterminous United States.  
1082 *Journal of Atmospheric and Oceanic Technology*, 38(11), 1979–1992.  
1083 <https://doi.org/10.1175/JTECH-D-21-0054.1>
- 1084 Lusardi, R. A., Hammock, B. G., Jeffres, C. A., Dahlgren, R. A., & Kiernan, J. D. (2019).  
1085 Oversummer growth and survival of juvenile coho salmon (*Oncorhynchus kisutch*) across a  
1086 natural gradient of stream water temperature and prey availability: An in situ enclosure  
1087 experiment. *Canadian Journal of Fisheries and Aquatic Sciences*, 1–12.  
1088 <https://doi.org/10.1139/cjfas-2018-0484>
- 1089 McGrath, E. O., Neumann, N. N., & Nichol, C. F. (2017). A statistical model for managing water  
1090 temperature in streams with anthropogenic influences. *River Research and Applications*, 33(1),  
1091 123–134. <https://doi.org/10.1002/rra.3057>
- 1092 Menne, M.J., Durre, I., Korzeniewski, B., McNeal, S., Thomas, K., Yin, X., Anthony, S., Ray,  
1093 R., Vose, R.S., Gleason, B.E., & Houston, T.G. (2012a). Global historical climatology network -  
1094 daily (GHCN-Daily), version 3.26. NOAA National Climatic Data Center.  
1095 <http://doi.org/10.7289/V5D21VHZ>. Accessed 2021-01-11
- 1096 Menne, M. J., Durre, I., Vose, R. S., Gleason, B. E., & Houston, T. G. (2012b). An overview of  
1097 the global historical climatology network-daily database. *Journal of Atmospheric and Oceanic*  
1098 *Technology*, 29(7), 897–910. <https://doi.org/10.1175/JTECH-D-11-00103.1>
- 1099 Moore, R. B., & Dewald, T. G. (2016). The road to NHDPlus—Advancements in digital stream  
1100 networks and associated catchments. *Journal of the American Water Resources Association*,  
1101 52(4), 890–900. <https://doi.org/10.1111/1752-1688.12389>

- 1102 Steel, E. A., Kennedy, M. C., Cunningham, P. G., & Stanovick, J. S. (2013). Applied statistics in  
1103 ecology: Common pitfalls and simple solutions. *Ecosphere*, 4(9), art115.  
1104 <https://doi.org/10.1890/ES13-00160.1>
- 1105 Stenhouse, S., Pisano, M., Bean, C., & Chesney, W. (2012). Water temperature thresholds for  
1106 coho salmon in a spring fed river, Siskiyou County, California. *California Fish and Game*, 98(1),  
1107 19–37.
- 1108 Welsh, H. H., Hodgson, G. R., Harvey, B. C., & Roche, M. F. (2001). Distribution of juvenile  
1109 coho salmon in relation to water temperatures in tributaries of the Mattole River, California.  
1110 *North American Journal of Fisheries Management*, 21(3), 464–470.  
1111 [https://doi.org/10.1577/1548-8675\(2001\)021<0464:DOJCSI>2.0.CO;2](https://doi.org/10.1577/1548-8675(2001)021<0464:DOJCSI>2.0.CO;2)
- 1112 Zillig, K. W., Lusardi, R. A., Moyle, P. B., & Fangue, N. A. (2021). One size does not fit all:  
1113 Variation in thermal eco-physiology among Pacific salmonids. *Reviews in Fish Biology and*  
1114 *Fisheries*. <https://doi.org/10.1007/s11160-020-09632-w>  
1115

1116 **Figure 1.** Klamath Basin study sites including the Scott River. Source map credits: Esri , NOAA,  
1117 and USGS.

1118

1119 **Figure 2.** Time series of (a) daily mean air temperature, (b) daily mean flow, (c) daily maximum  
1120 stream temperature ( $T_{\max}$ ), and (d) daily mean stream temperature ( $T_{\text{mean}}$ ) at Scott River from  
1121 1998–2020.

1122

1123 **Figure 3.** Inputs to Scott River “quantile air temperature” scenarios representing 15  
1124 combinations of (a) three air temperature inputs and (b) five flow inputs that vary by day.  
1125 Observed values for 1998–2020 are shown as gray lines.

1126

1127 **Figure 4.** Model formulas and summary of RMSE from extrapolation and LOYO CV tests at 10  
1128 Klamath Basin sites applying  $T_{\max}$  (top panels) and  $T_{\text{mean}}$  (bottom panels) models to years  
1129 (LOYO) or flow and air temperature combinations (extrapolation) not used in model calibration.  
1130 Models are sorted by overall RMSE rank (i.e., mean rank of all 10 sites and both temperature  
1131 metrics, Table S2). Extrapolation test RMSE values for top eight models in individual site panels  
1132 are labeled, with asterisk marking lowest RMSE in each panel. Formulas for  $T_{\max}$  and  $T_{\text{mean}}$   
1133 models are identical, so are only listed once. Key to formulas: D = day of year from 1 (1  
1134 January) to 366 (31 December in leap year); Q = daily mean flow; see Section 3.1.2 for key to  
1135 ‘A’ air temperature variables; ‘s()’ is a nonlinear function; ‘s(D, by =)’ is a linear interaction that  
1136 varies smoothly by D; ‘te()’ is a fully nonlinear tensor product smooth of two or three variable;  
1137 and ‘ti()’ is a tensor product interaction. Except GAM11, all models also include an AR1  
1138 autocorrelation structure and random effect of year.

1139

1140 **Figure 5.** Configuration of data blocks used in extrapolation tests for model selection and  
1141 validation.

1142

1143 **Figure 6.** Effects of flow (Q) and day of year (D) on predicted values of (a)  $T_{\max}$  and (b)  $T_{\text{mean}}$  in  
1144 Scott River GAM7. Colors and labeled contour lines show predicted temperatures ( $^{\circ}\text{C}$ ).  
1145 Underlying gray dots show calibration data.

1146

1147 **Figure 7.** Modeled Scott River  $T_{\max}$  and  $T_{\text{mean}}$  under the 15 “quantile air temperature” scenarios  
1148 representing combinations of three air temperature inputs (arranged in columns) and three  
1149 quantile flow inputs and two management flow inputs (shown by color). Observed values for  
1150 1998–2020 are shown as gray lines. Selected data values are labeled on 15 June and the first day  
1151 of March–October. Horizontal dashed line is the salmonid temperature threshold.

1152

1153 **Figure 8.** Modeled stream temperature differences between lowest flow (0.1 quantile) and  
1154 highest flow (0.9 quantile) scenarios throughout the year for (a)  $T_{\max}$  and (b)  $T_{\text{mean}}$  at 10 Klamath  
1155 Basin sites estimated using GAM7.

1156

1157 **Figure 9.** (a) Annual maximum stream temperature, (b) annual degree-days exceeding 22 °C,  
1158 and (c) first and (d) last day when  $T_{\max}$  exceeded 22 °C in Scott River model scenarios pairing  
1159 observed air temperatures with eight flow scenarios. Means of all years are shown with black  
1160 points and grey “x” show individual years, offset for clarity.

1161

1162 **Table 1.** Matrix showing model scenarios representing combinations of air temperature and flow  
 1163 inputs, and organized into two scenario groups. The first group (15 scenarios) used “quantile air  
 1164 temperature” inputs (6 were only run only at Scott River while 9 were run at all Klamath Basin  
 1165 sites) and the second group (8 scenarios) were run only at Scott River and used “observed air  
 1166 temperature” inputs.  
 1167

Scenario group	Air temperature inputs	Flow inputs							
		Lowest (0.1 quantile)	Typical (0.5 quantile)	Highest (0.9 quantile)	USFS water right	CDFW flow criteria	Observed	Maximum of observed or USFS	Maximum of observed or CDFW
Quantile air temperature	Hottest (0.9 quantile)	All sites	All sites	All sites	Scott only	Scott only			
	Typical (0.5 quantile)	All sites	All sites	All sites	Scott only	Scott only			
	Cooltest (0.1 quantile)	All sites	All sites	All sites	Scott only	Scott only			
Observed air temperature	Observed (measured on date)	Scott only	Scott only	Scott only	Scott only	Scott only	Scott only	Scott only	Scott only

1168

Figure 1.

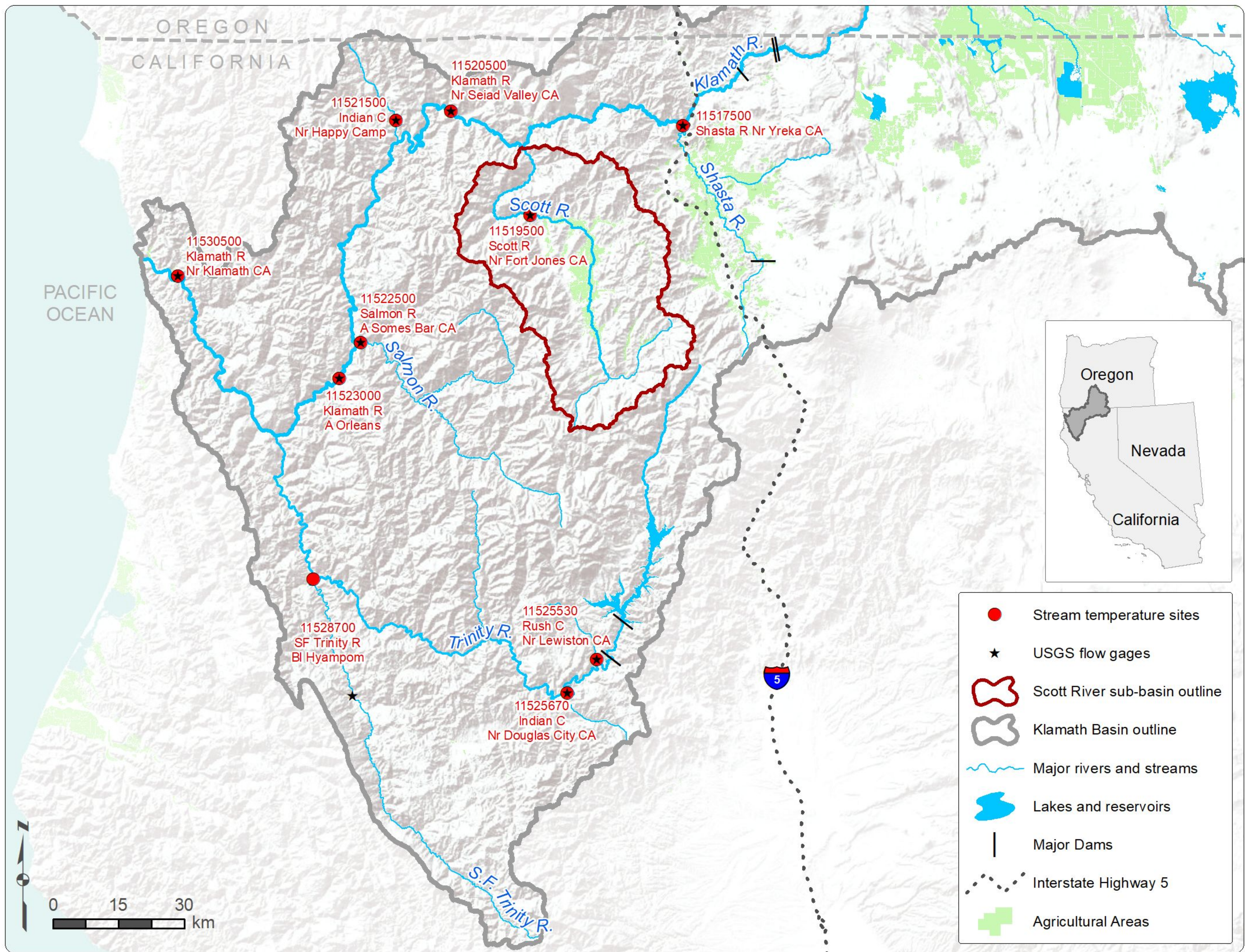


Figure 2.

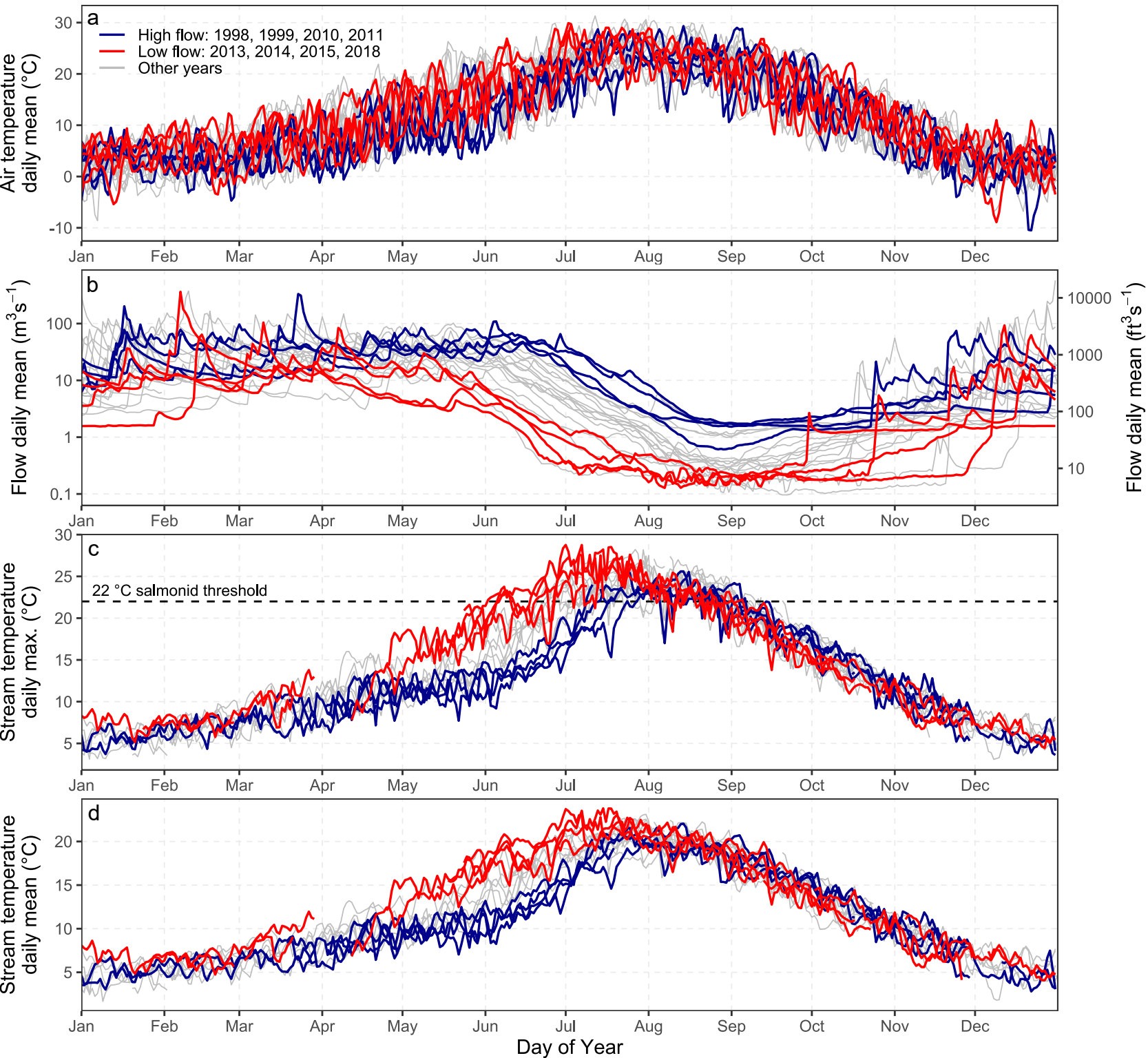


Figure 3.

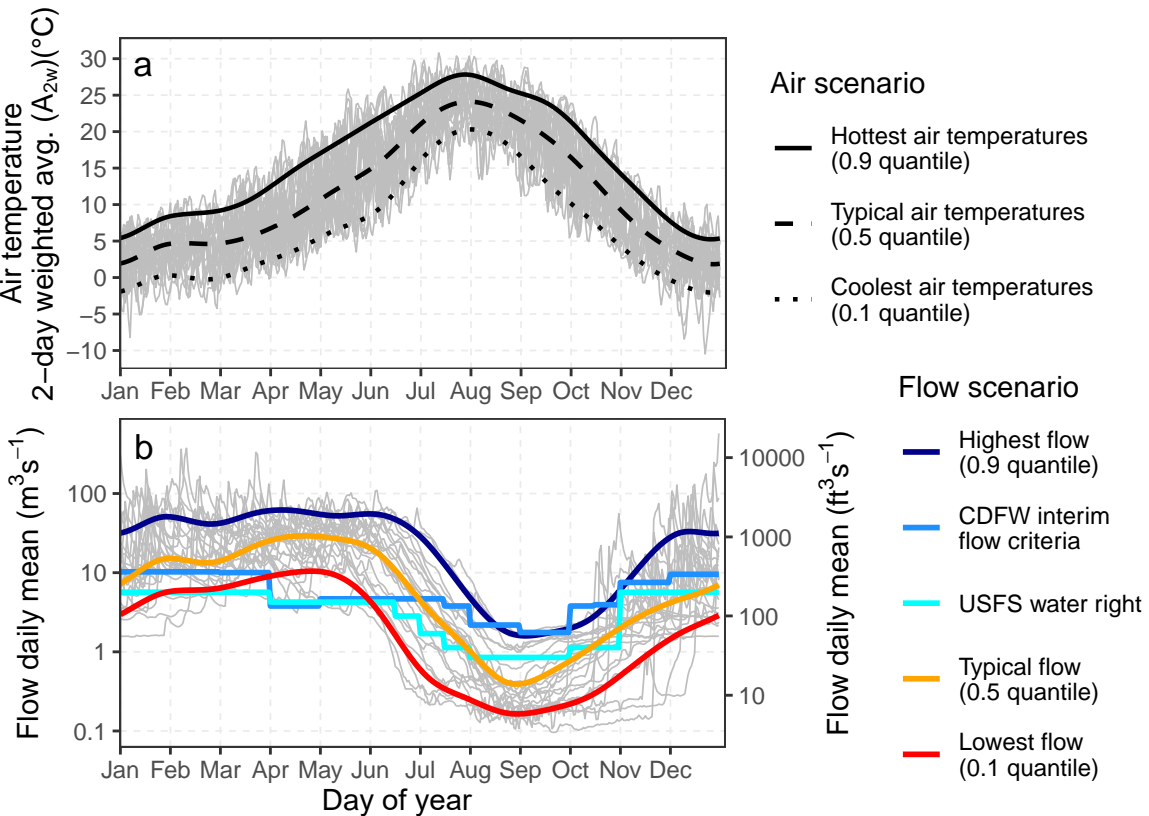
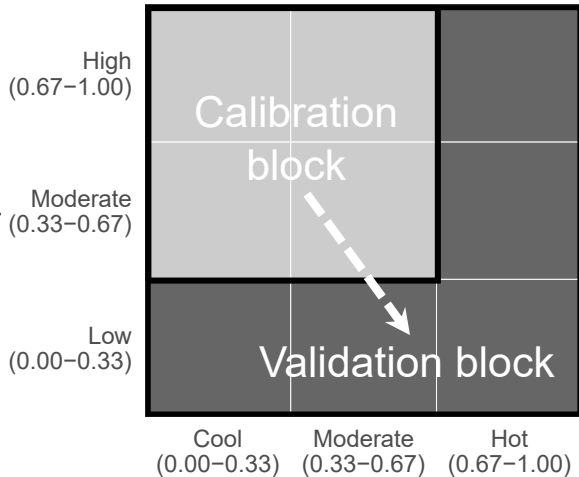


Figure 4.

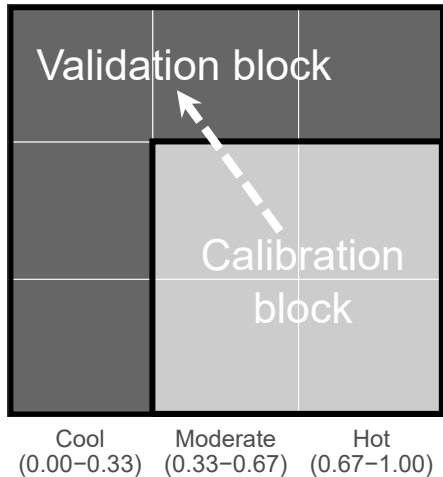


Figure 5.

Predict Low-flow and/or Warm days  
from  
High-flow, Moderate, and/or Cool days



Predict High-flow and/or Cool days  
from  
Low-flow, Moderate, and/or Warm days



Air temperature quantile

Figure 6.

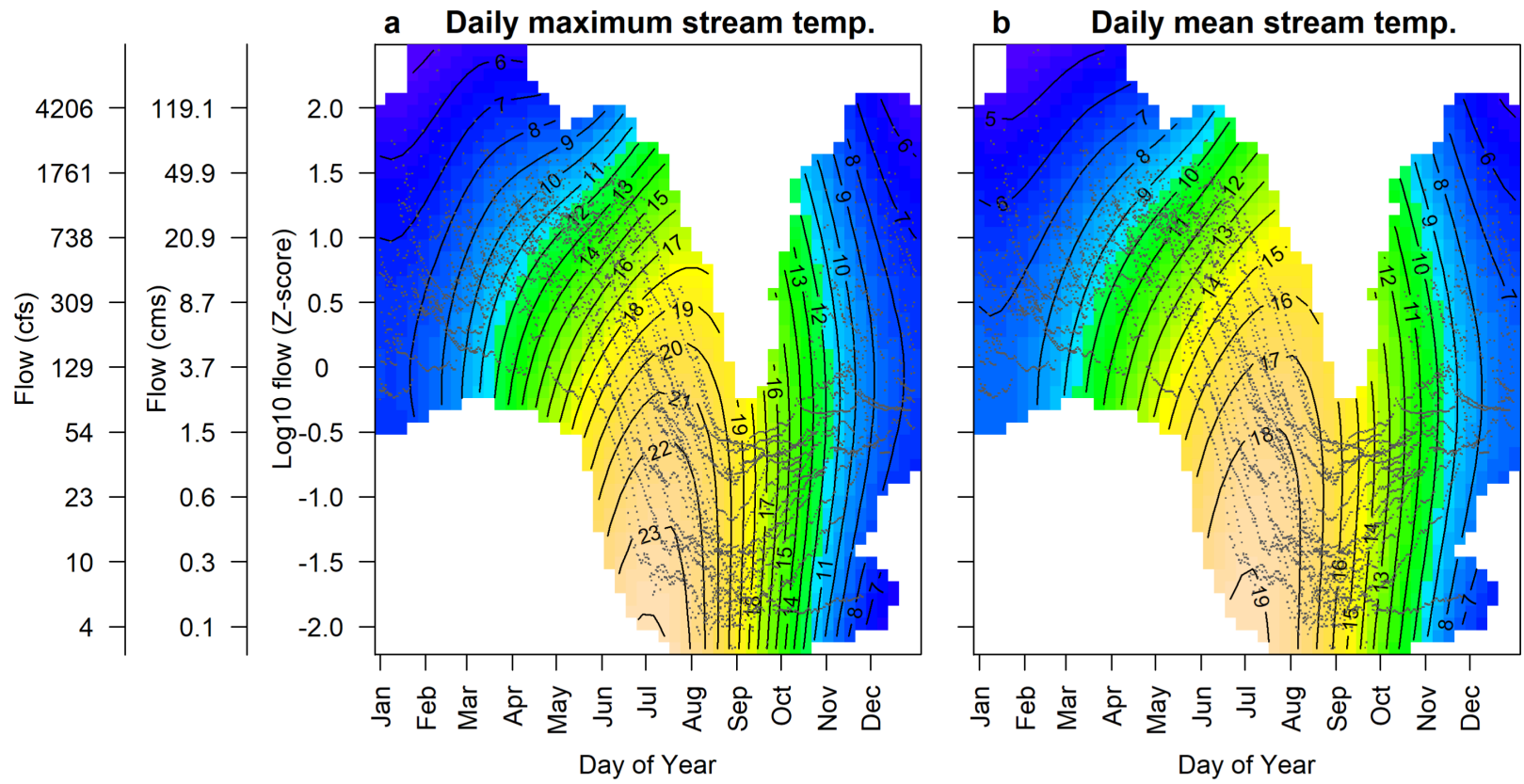


Figure 7.



Figure 8.

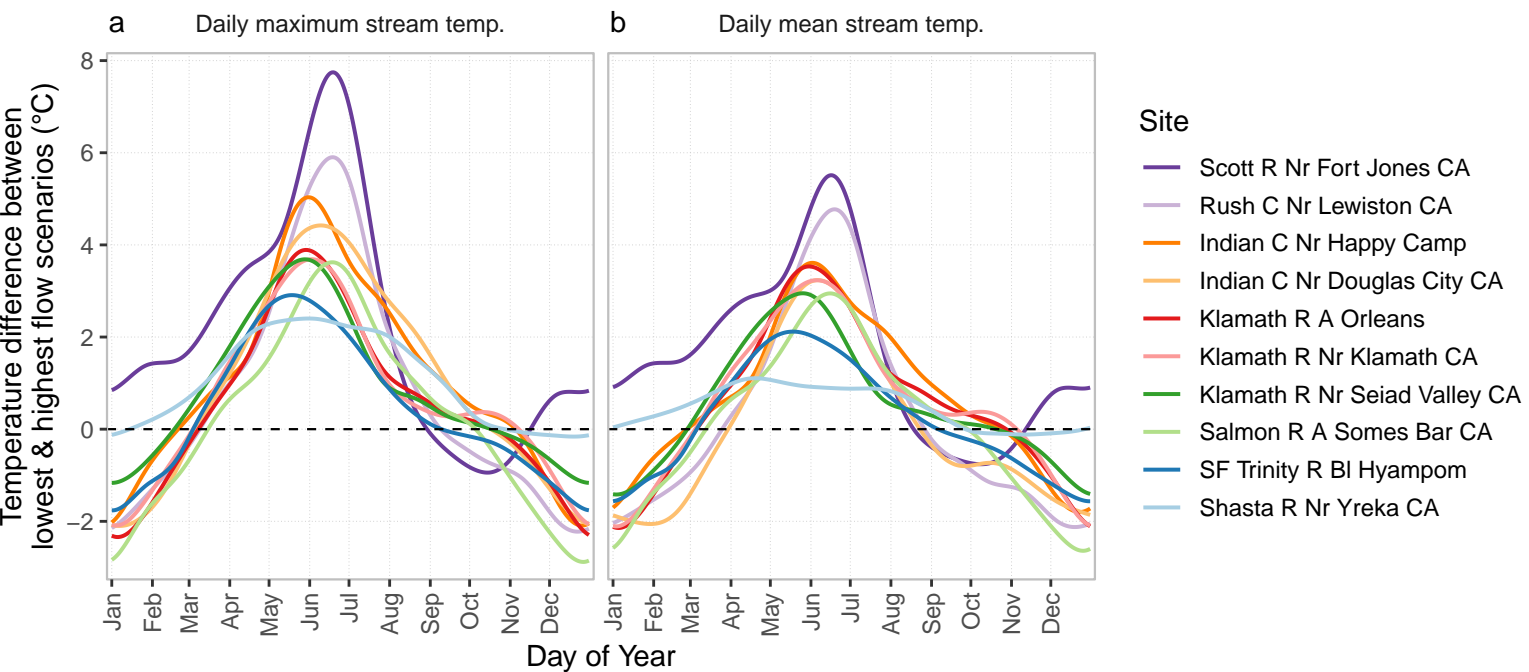


Figure 9.

